# Network Topology of the Interphase between Cross-Linked Polyurethane/Ethylene Propylene Diene Terpolymer Elastomers for Adhesion Applications

Nancy Desgardin, Agnès Aymonier, Cédric Lorthioir

# Network Topology of the Interphase between Cross-linked Polyurethane/Ethylene Propylene Diene Terpolymer Elastomers for Adhesion Applications

*Nancy Desgardin[1,*], Agnès Aymonier[1], Cédric Lorthioir[2,*]*

(1) ArianeGroup, Centre de Recherches du Bouchet, 91710 Vert-le-Petit, France

(2) Sorbonne Université, CNRS, Laboratoire de Chimie de la Matière Condensée de Paris, LCMCP, UMR 7574, 75005 Paris, France

KEYWORDS:

polyurethane, network topology, interfaces, elastomer bonding, solid-state NMR

ABSTRACT:

Understanding the interfacial phenomena involved in the adhesion between elastomer layers on a molecular basis is an important topic from both fundamental and applied aspects.

Nevertheless, this topic has been poorly addressed experimentally. This report aims at rationalizing differences in the adhesion behavior of polyurethane (PU) elastomers cured on an ethylene-propylene-diene terpolymer (EPDM) substrate, based on a detailed description of their local network-like topology, determined thanks to $^{1}H$ solid-state nuclear magnetic resonance (NMR) spectroscopy. The polyurethanes, composed of the same fraction of hydroxy-terminated poly(butadiene) and isophorone diisocyanate, were cured under different reaction conditions – nature and concentration of the catalyst as well as the crosslinking temperature. The rigid domains formed by the hard segments, the proportion of elastically-active chains and the distribution of the topological constraints in the soft domains were investigated by $^{1}H$ solid-state NMR, taking advantage of magic sandwich echoes and double quantum-based experiments. The PU network topology within 20 μm-thick slices collected near the interface with the EPDM layer was systematically compared to the one observed for 60 μm-thick slices, located 500 μm from the interface, corresponding to bulk regions. Curing at low temperature (30°C) with a low amount of catalyst (0.02 wt %) leads to elastically-active poly(butadiene) chains close to the interface with, on average, higher molecular weights between topological constraints than the ones in the bulk. Such differences between interfacial and bulk regions are not observed any longer as the catalyst concentration is increased to 0.2 wt %. These variations of the local PU network topology, occurring over several tens of micrometers, allow to account for the adhesion testing results.

## 1. INTRODUCTION

Adhesion phenomena play a crucial role in various fields of applications in materials science or biophysics/bioengineering for instance. However, adhesion mechanisms are intrinsically complex and as a result, the processes involved are often difficult to model. Interestingly, it was realized some years ago that the adhesion between soft polymer materials, among which cross-linked elastomers, had been poorly investigated in the past.[1] Experimental works were dedicated to a detailed characterization of the adhesion behavior between two chemically-distinct elastomers, using mechanical testing (peel or lap shear tests for instance). Some attempts were more recently proposed to rationalize the adhesion behavior on the basis of molecular/macromolecular arguments,[2,3] despite the relationships between the macroscopic and the microscopic behaviors are not easy to derive from an experimental point of view.[4] Along this line, Yu *et al.* performed careful measurements of both work of adhesion and work of separation for non-extracted and extracted silicone networks, with various cross-link densities.[5] In this contribution, attempts to account for the different adhesion strengths of the systems investigated were proposed. In particular, the authors used the fraction of free or dangling chains at the surfaces of both silicone components to rationalize the differences in the work of adhesion and the work of separation among the networks considered. However, the amount of both free chains and dangling chains near the interfaces was not experimentally determined. Such a measurement is indeed very difficult, if not impossible, to fulfill since it would assume the detection of a very weak amount of chain portions. Nevertheless, establishing correlations between the macroscopic adhesion behavior of two elastomers and parameters related to the network topology in the interfacial regions, such as the fraction of dangling (or elastically-active) chains or the local cross-link density, is an appealing approach that should help to derive models to describe and predict the adhesion behavior. To the best of our

knowledge, such an experimental approach has not yet been used in the field of elastomer adhesion. This contribution aims at establishing the proof of concept of such an approach, using the interphase between EPDM (a terpolymer based on ethylene, propylene and diene units) and a polyurethane (PU) elastomer.

EPDM/polyurethane elastomer interfaces indeed play an important role for several important applications in both automotive and aerospace industries and in particular, in the design of solid propellant rocket case.[6] In such systems, the propellant is converted into gaseous combustion products displaying a high temperature. The cross-linked EPDM component, usually containing filler particles, thus acts as a thermal insulation layer allowing to protect the case while the PU component serves as a binder between the EPDM layer and the solid propellant. Adhesion should be high enough between both EPDM and PU components, in order to keep the combustion profile unchanged. PU elastomers are usually selected for such applications because they offer a wide range of chemical structures for both hard segments (HS) and soft segments (SS). Besides, they can be synthesized from liquid precursors, at room temperature, and without any resulting by-products.[7] Nevertheless, the various reactions between the isocyanate and the polyol precursors are known to be highly sensitive to the experimental conditions such as the reaction time, the reaction temperature or the nature and amount of catalyst. These preparation conditions are expected to influence the topology of the network resulting from the reactions of the hydroxyl groups of the polyol chains with the isocyanate ones. One possibility to design new PU elastomers with satisfactory adhesion with EPDM substrates relies on a systematic testing of their adhesive behavior, using peel tests or tension pull tests for instance. Another possibility is to determine the influence of the PU network topology on the adhesion with the EPDM layer and, in particular, the

influence of the fraction of elastically-active chains (as well as the fraction of dangling chains and the one of free chains) in the interfacial regions.

Beyond the fractions of elastically-active chains near the interfaces, another important feature to be considered is the distribution of the cross-link density for each of both layers in contact, evaluated once again within the interphase. Indeed, such a macromolecular parameter also contributes to the elastic modulus of the interfacial regions and thus, should influence the adhesion behavior. It may be tempting to consider that the cross-link density in the PU interphases is similar to the one of the bulk materials, prepared under similar experimental conditions than the PU formed after deposition on the EPDM layer. However, depending on the kinetics of the PU's formation, diffusion of the liquid PU precursors towards EPDM may occur and the local composition near the interface might differ from the initial one. Such a feature may induce a different network topology in the interphase, which may influence the adhesion behavior. Under these conditions, an experimental approach allowing to determine selectively the local cross-link density at the interphase of EPDM/PU systems would be required.

Solid-state NMR has proven to be a powerful tool to study both chemically- and physically-cross-linked elastomers over various length scales.[8,9] Beyond the spectroscopic approaches that allow to monitor the evolution of the chemical structure of the network chains at the molecular scale during cross-linking or aging for instance,[10] time-domain NMR may provide complementary information on the network topology, at the chain level.[11–13] In this contribution, solid-state NMR is used to investigate the PU network topology in the interfacial region of cross-linked elastomers in contact, EPDM and PU, in order to get a deeper understanding of the adhesion behavior between both components. In particular, the fraction of repeat units involved in free, dangling and elastically-active chains near the interfaces as well as the distribution of the cross-link density will

be determined and compared to the same parameters, determined in the bulk, further from the EPDM/PU interfaces. The influence of the reaction conditions on the PU network (temperature, nature of the catalyst, amount of catalyst) was assessed for both interfacial and bulk-like regions and these results allowed to understand the adhesion performances of these various materials. The experimental approach proposed here relies on $^{1}$H solid-state NMR – $^{1}$H transverse relaxation[14,15] and $^{1}$H double quantum-based experiments[12,13] – which are intrinsically highly sensitive and as a result, may be applied with a rather low amount of samples. This feature indeed makes possible the distinction between the interphases and the bulk regions, located far from the interfaces.

## 2. MATERIALS AND METHODS

### 2.1. Materials

The preparation of the polyurethane materials involves several alcohols: one polyol, a hydroxyl-terminated poly(butadiene) prepolymer (HTPB), and two low-molecular-weight alcohols (chain-extender alcohols). HTPB was the polyol selected to prepare the PUs considered in this work because the aim was to investigate EPDM/PU assemblies that are currently used in the aerospace industry and in particular, in the design of solid propellant rocket cases. For this application, a PU elastomer serves as a liner between the thermal insulator (EPDM) and the propellant. As most of the composite propellants are based on HTPB, this latter is also used for the design of the PU liner, thus allowing to enhance the compatibility with the propellant binder and therefore, the bonding between both components, PU and propellant.

HTPB was purchased from Cray Valley under the reference Poly bd® R45 HTLO and used without further purification. Its number-average molecular weight and its polydispersity index, as

determined by size exclusion chromatography, are equal to $M_n$ = 2900 g.mol$^{-1}$ and *PDI* = 1.8 while its functionality was estimated to 2.5 by potentiometry[16]. Isophorone diisocyanate (IPDI) was obtained from Evonik and served as a curing agent. Its purity was higher than 99.5 wt %, as determined by gas chromatography. The NCO/OH molar ratio was set to 1. In order to obtain a shear-thinning material in the non-cured state, required for its spraying on thermal insulation layers (EPDM sheets) used in the industrial production of rocket cases, this mixture is filled by carbon black, with a filler content of 12 wt %. Additives (antioxidant, adhesion promoter, catalysts) amount to less than 5 wt % of the whole formulations. The chemical structure of these additives as well as the one of the two chain-extender alcohols are not reported, for the sake of confidentiality.

Four polyurethanes prepared with the same HTPB, the same chain extenders and IPDI, all used in the same proportions, were considered in order to assess the possibility to perform the curing process at room temperature thanks to a new catalyst. In particular, the efficiency of this latter will be compared to the one observed using a reference one. The conditions used for the preparation of these polyurethanes are reported in **Table 1**. The hydroxyl-terminated poly(butadiene) prepolymer, the low-molecular-weight alcohols (chain extenders), carbon black and the additives were degassed and mixed at 65°C under vacuum for 4 hours. After cooling down to room temperature, both isophorone diisocyanate and catalyst were added and a mixing of 20 minutes was carried out, again under vacuum. The mixture was poured either on a non-stick mold or on an EPDM substrate with a thickness of 1 mm and then cured at 65°C or 30°C. Both surface composition and morphology of the EPDM sheet, which are important parameters, have been characterized. In particular, the FTIR spectrum, obtained using the ATR mode with a germanium crystal, and XPS data are reported in **Figure S1**.

| Sample name | Catalyst | Catalyst content | Curing temperature | Duration | Extractable fraction | Swelling Ratio |
|---|---|---|---|---|---|---|
| **PU0** | Reference | 0.04 wt % | 65°C | 7 days | 14 % | 4.7 |
| **PU1** | New | 0.02 wt % | 65°C | 7 days | 15 % | 5.1 |
| **PU2** | New | 0.02 wt % | 30°C | 2 months | 22 % | 6.2 |
| **PU3** | New | 0.2 wt % | 30°C | 2 months | 34 % | 8.5 |

**Table 1.** Curing conditions, extractable fraction and swelling ratio at equilibrium of the four polyurethane materials.

### 2.2. Rheology

The viscosity increase of the HTPB/chain extenders/IPDI mixtures over curing at a given temperature was monitored with a rotational rheometer (Bohlin rheometer CVOR 120) equipped with a cone-plate geometry (40 mm cone diameter, 4° cone angle). The measurement conditions were identical for all the investigated materials: the shear rate was set to 0.215 $s^{-1}$ and one measurement was performed per hour during 24 hours.

### 2.3. Swelling measurements

After curing, samples of initial weight $w_i$ (about 3 g typically) were swollen in toluene, which is known to be a good solvent of poly(butadiene). The sample weight at the swelling equilibrium, $w_s$, and the one after subsequent drying (1 week in a fume hood), $w_d$, were determined, allowing to calculate both the swelling ratio $Q = w_s/w_d$ and the extractable fraction, $(w_i-w_d)/w_i$.

### 2.4. Mechanical tests

The mechanical tests described below are performed to assess the performances of the prepared polyurethane materials regarding acceptance tests.

Tensile tests were performed on films corresponding to a 1 mm-thick tensile specimen standard H2, using a single-column Zwick-Roell Z 1.0 machine with grip roll. The strain rate was set to 50 mm/min and the temperature was regulated at 20°C. Measurements were averaged over 5 H2 specimens for each material.

Adhesive properties were evaluated by means of tensile tests carried out on EPDM/polyurethane cylindrical samples (diameter of 25 mm, EPDM thickness equal to 5 mm, polyurethane thickness of 1 mm, see Supplementary Information, **Figure S2**). For these experiments, the PUs were prepared according to the protocol described in Section 2.1 and after curing, samples with a cylindrical shape were die-cutted, the axis of the cylinders corresponding to the normal to the EPDM and PU layers. The strain rate was fixed to 10 mm/min and the temperature was kept at 20°C. For each system, 3 separate experiments were systematically performed.

### 2.5. $^{1}$H solid-state NMR

The $^{1}$H solid-state NMR experiments were carried out on a 300 MHz Bruker Avance III HD spectrometer, with a 4 mm $^{1}$H-X double-resonance MAS probe used under static conditions. The sample temperature was maintained at 80°C. The 90°($^{1}$H) pulse length $t_{90°}$ was equal to 2.54 μs and the recycle delay was fixed to 3 s, which is higher than 5 times the relaxation time $T_1$($^{1}$H) of the samples investigated, at 80°C.

The $^{1}$H transverse relaxation functions were determined in the short-time regime (0 – 200 μs) using the Magic-Sandwich Echo (MSE) experiment.[15,17] The $^{1}$H multiple-quantum (MQ) build-up curves were recorded using the approach developed by Saalwächter et al.[12,13] For this purpose, both the multiple-quantum (MQ), mostly double-quantum (DQ), coherences and the reference

signal were monitored as a function of the excitation time, $t_{exc}$. This latter was chosen as a multiple of the cycle time $t_c$, equal to 154 μs in the present case. Besides, the finite length of the $^1$H pulses was taken into account by rescaling the $t_{exc}$ values by the factor $(1 - 12 \times t_{90°}/t_c)$, thus leading to the effective $^1$H DQ excitation time, $t_{DQ}$.

These experiments were performed on 10 – 20 mg of polyurethanes. In particular, slices from the cylinder-shaped samples used to test the adhesive properties were cut with a microtome, perpendicular to the cylinder axis, within the 1 mm-thick PU layer cured on the EPDM sheet. The slice thickness was adjusted to 20 μm when collected near the interface with the EPDM substrate and 60 μm when collected in the bulk polyurethanes, as schematically illustrated in **Figure S2**. At this stage, it should be emphasized that here, the term "bulk" refers to PU samples microtomed in the 1 mm-thick PU layer, but far (about 500 μm) from the EPDM/PU interface.

## 3. RESULTS

### 3.1. Kinetics of urethane group formation

The time evolution of the viscosity was measured for each HTPB/chain extenders/IPDI mixture, during the curing process, as shown in **Figure 1**. As expected, the viscosity is found to raise up over time during curing, as a result of the formation of urethane groups. The time evolution observed for the polyurethanes prepared at 65°C (PU0 and PU1) displays at least two stages over the probed time range, which are assumed to result from the different alcohol and isocyanate functions present in the formulation. Such a feature has already been observed for HTPB/IPDI systems.[18] HTPB, obtained by free-radical polymerization, indeed displays a functionality higher than 2 (2.5 in the present case) and the corresponding hydroxyl groups are involved in primary

functions among which hexene-2-1-type, vinyl-type and geraniol-type OH (**Scheme S1**), as evidenced by $^{1}H$ and $^{13}C$ solution-state NMR. As expected, the reactivities of such hydroxyl functions were shown to be significantly different.[19] Besides, the secondary NCO group of IPDI also displays a higher reactivity than the primary one.[20] Lastly, the reactivities of the hydroxyl functions from the chain extender alcohols should also be considered and add further complexity. Concerning PU2 and PU3, only one stage may be observed over the probed time range (**Figure 1**).

Compared to the reference formulation PU0, the kinetics of the viscosity increase at 65°C is faster for the composition PU1, which is prepared with a different catalyst, although this latter was present in lower concentration than the one used for PU0. When the curing process is performed at lower temperature (30°C) on a mixture identical to PU1, the viscosity increases much more slowly, in comparison to PU1 (See **Figure 1**, PU2). Nevertheless, when the catalyst content is ten times higher than for PU2 (system PU3), the kinetics of the viscosity increase at 30°C gets faster than for PU2 and interestingly, even faster than for the reference material PU0, though cured at 65°C. These results indicate that the pot life may be tuned with both temperature and catalyst content.

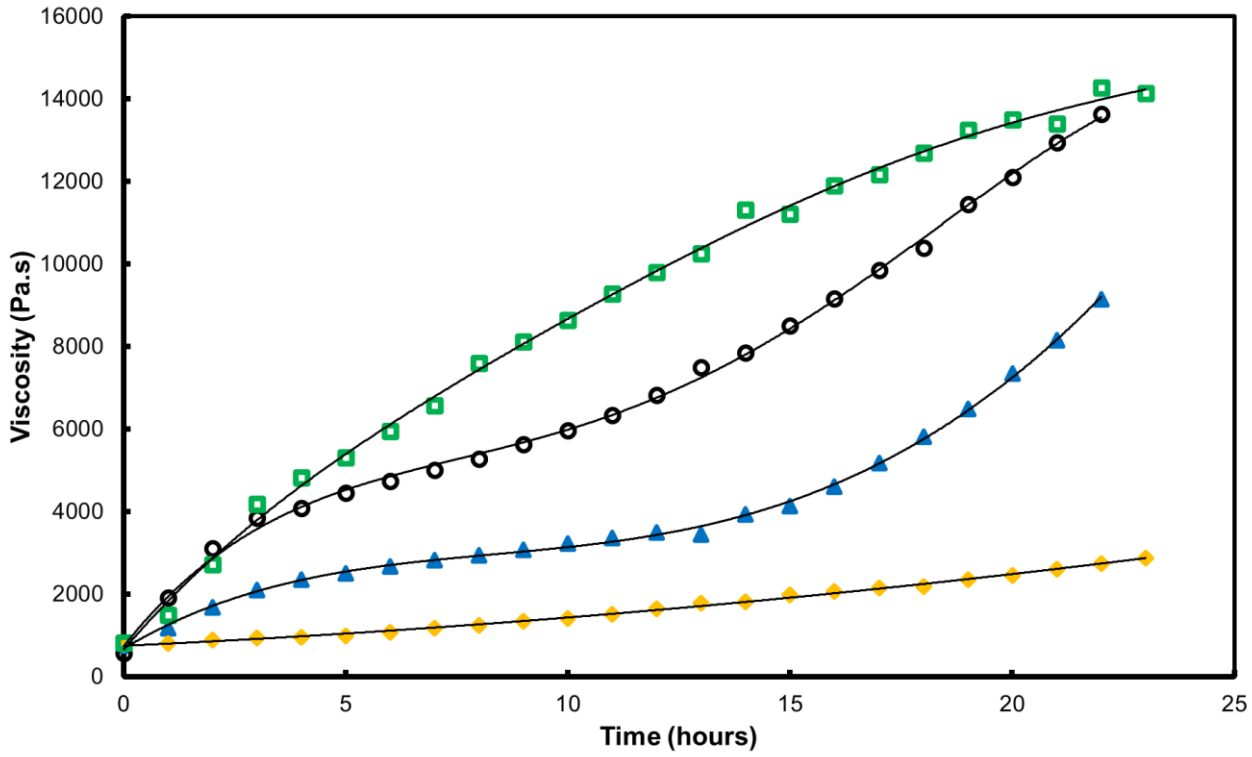


**Figure 1.** Viscosity increase for PU1 (○), PU2 (◆) and PU3 (□) over curing. Data obtained for the reference system, PU0 (▲), are included for the sake of comparison. The curing conditions are indicated in **Table 1**.

### 3.2. Polyurethane network topology: swelling measurements

The swelling ratio at equilibrium, Q, and the extractable fraction were determined for each of the four polyurethane materials investigated in this study and the results are reported in **Table 1**. The relatively high value of the extractable fraction,[21] although the initial NCO/OH molar ratio was equal to 1, may be assigned to the fact that the considered HTPB contains a non-negligible fraction of monofunctional chains, with a hydroxyl group at a single of both chain ends, due to the

method used for its synthesis:[16] such a OH group may not allow the chain to be linked to the network and then, the corresponding chain contributes to the extractable fraction.

PU1 and PU0, which only differ by the chemical nature of the catalyst used for the curing process, are characterized by very similar values of both swelling ratio Q and extractable fraction. The comparison between the data related to PU2 and PU1 suggests that when the curing process is performed at 30°C, the resulting network displays a higher swelling ratio and should thus be less cross-linked than for PU1. Such a trend should origin from the effect of the side reactions as the temperature is decreased.[22] These latter typically consist of reactions of isocyanate groups with moisture that decrease the chemical crosslink density. Moreover, **Table 1** indicates that the curing at 30°C, carried out with a higher amount of catalyst in the initial mixture (concentration multiplied by 10), does not allow to reduce the measured swelling ratio compared to the one obtained for PU2.

### 3.3. Mechanical tests

Tensile tests carried out on the PU films, prepared without any EPDM substrate, are reported in **Figure 2**. From a qualitative point of view, all the stress-strain curves display a similar rubber-like profile.[4] The data obtained for PU0 and PU1 are nearly identical and in particular, the secant modulus at 50 % strain for instance is the same for both samples (3.0 MPa), in agreement with the similar value of their swelling ratio at equilibrium. The stress-strain curves of both polyurethanes PU2 and PU3 are also quite close, especially in the low deformation regime, in which a secant modulus at 50 % strain of about 1.9 MPa – 1.5 times lower than the one determined for PU0 and PU1 – is observed. Therefore, both PU2 and PU3 display poorer mechanical performances than PU0 and PU1. Such a decrease is also consistent with the swelling measurements: for PU2 and PU3, Q was indeed found to be lower than the values measured for PU0 and PU1.

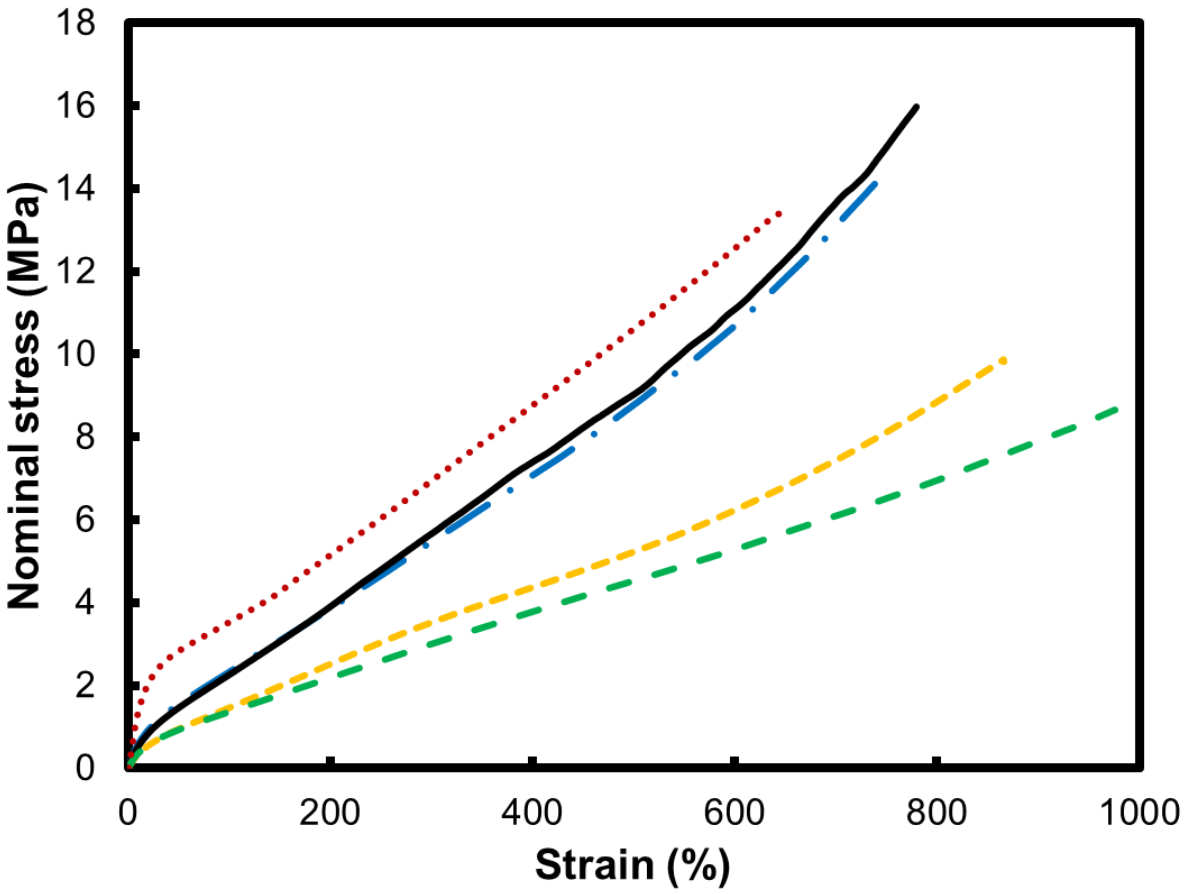


**Figure 2.** Tensile tests for PU0 (——-), PU1 (——), PU2 (- - -) and PU3 (– – –), formed in a mold, without any EPDM layer. The stress-strain curve obtained, under the same experimental conditions, for the EPDM sheet used, in the following, as a substrate to prepare the PU elastomers is included in the plot, for the sake of comparison (• • • •).

Tensile tests on EPDM/PU cylindrical samples are presented in **Figure 3**. The first part of the curves (strain lower than 5 %) corresponds to the elastic deformation, occurring mostly within the PU component since this latter is a softer material than the considered amorphous EPDM elastomer. The secant modulus at 50 % strain of this EPDM substrate is indeed found to be about 5.7 MPa, as can be seen on **Figure 2**. **Figure 3** shows that as the strain is further increased, the

stress reaches a maximum, corresponding to the onset of the cavitation within the PU.[23] The cavitation is followed by the deformation of fibrils until debonding. Both stress-strain curves obtained with PU1 and PU3 are close to the one determined for the reference system (PU0) and from the industrial point of view, these materials meet the bonding specifications. Though displaying a similar elastic deformation behavior as PU3 (**Figure 2**), a worse behavior is observed for PU2, as far as the bonding properties are concerned. The results deduced from a quantitative analysis of the adhesion tests carried out for three specimens of each of the four EPDM/PU samples are reported in **Table S1**.

At this stage, it should be noted that the comparison of the relative position between the strain-stress curves reported in **Figure 2** and **Figure 3** may be delicate to discuss for several reasons. Due to the intrinsic difference between both kinds of mechanical tests used (uniaxial tension and poker-chip experiments), the strain distribution within the specimens and the nature of the measured apparent modulus are not the same. Moreover, the apparent modulus determined in the uniaxial tension experiments (**Figure 2**) is related to the PU component only whereas the tensile tests shown in **Figure 3** involve the apparent modulus of EPDM/PU assemblies (see **Figure S2**) and are thus related, but not equal, to the modulus which would be obtained with a poker-chip of neat PU or neat EPDM. Lastly, the strain rate for both sets of tests are significantly different (50 mm/min for the uniaxial tension tests and 10 mm/min for the poker-chip experiments).

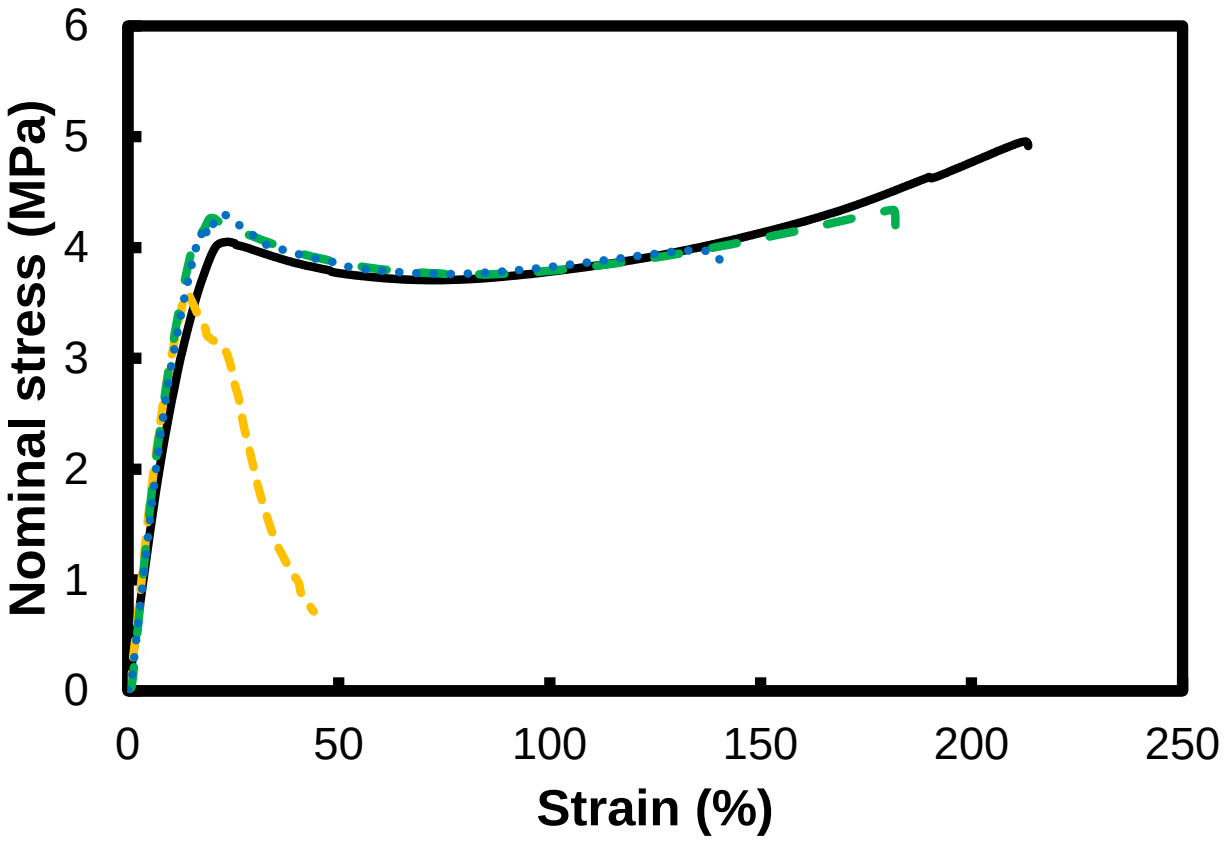


**Figure 3.** Tensile tests on EPDM/PU cylindrical samples performed for PU0 (—— -), PU1 (——), PU2 (- - -) and PU3 (– – –).

The results of the acceptance tests reported in **Figure 2** and **Figure 3** allow to optimize the experimental conditions to be used to form polyurethanes with satisfactory mechanical properties, in regard of their targeted application. Thus, when the new catalyst is chosen for preparing the polyurethanes at 30°C, PU2 and PU3 are found to display rather similar stress-strain curves under uniaxial deformation whereas the amount of catalyst required to achieve adhesive properties similar to the one of the reference material (PU0) should be much higher than 0.02 wt % (PU2): it may be, for instance, equal to 0.2 wt % (PU3). However, the understanding of such differences in

the mechanical behavior requires to investigate these systems at the macromolecular length scale and therefore, in the following, the network topology within these polyurethanes will be probed.

### 3.4. Polyurethane network topology far from the EPDM interface: $^{1}$H solid-state NMR

#### 3.4.1. Network-like structure of bulk PU1

The polyurethanes considered in this work, prepared with IPDI as a diisocyanate, were found to display a significant extent of phase separation between HS and SS. Nevertheless, Kojio *et al.* have recently reported that the symmetry of the chemical structure of the diisocyanate plays a very important role on the degree of phase separation in polyurethanes: a high symmetry of the diisocyanate tends to promote the formation of hydrogen bonds between the HS and in some cases, their crystallization, thus resulting in a higher degree of phase separation.[24] From this point of view, IPDI corresponds to an asymmetric and bulky structure. This feature, combined to the occurrence of two stereoisomers, should make the ordering of the HS more difficult within the polyurethanes investigated here. For these latter, the HS were anyway found to aggregate significantly, as evidenced by FTIR experiments performed on a polyurethane of the same composition.[25] These measurements demonstrated that the percentage of hydrogen-bonded N-H functions amounts to about 90 % while the one of the carbonyl groups is estimated to about 97 %. The high percentages of bonded N-H and bonded C=O determined for this polyurethane, together with their similar value, indicate that a significant aggregation of the HS occurs in this material: an important degree of microphase separation is thus observed. Despite the asymmetry of IPDI, such an aggregation of the HS is driven by the fact that HTPB is a non-polar prepolymer: under these conditions, the polar HS which contain the urethane groups and the short-chain diols strongly tend to interact, thus forming the so-called "rigid domains".

The polyurethane network topology was investigated by complementary $^{1}H$ solid-state NMR approaches. The $^{1}H$ transverse relaxation signal was first determined in the short-time regime, which corresponds to 0 – 200 μs in the present case. For this purpose, the Magic Sandwich Echo pulse sequence was used. The result obtained on the PU1 material far from the EPDM layer is depicted in **Figure 4**. A fast-relaxing component is detected over the first 20 microseconds, indicating the presence of protons involved in strong $^{1}H$-$^{1}H$ dipolar couplings, which are not efficiently averaged by molecular reorientations. Such protons should correspond to the ones involved in the domains formed by the HS within this polyurethane. From this point of view, this NMR experiment thus leads to a two-phase description of PU1, which is consistent with the microphase separation scheme previously evidenced by FTIR. As shown in **Figure 4**, a satisfactory fit of the experimental data could be performed using the following expression:

$$\frac{M(t)}{M_0} = f_H \times e^{-\frac{a \times t^2}{2}} + (1 - f_H) \times e^{-\frac{q.M_2 \times t^2}{2}} \times e^{-\frac{t}{T_2}} \qquad (1)$$

$f_H$ denoting the fraction of protons present in the rigid domains and a, the fit parameter aimed at describing the fast-relaxing component. The first term of eq 1 corresponds to the protons from species which are immobile, or nearly immobile, over a few tens of microseconds. In the context of phase-separated polyurethanes, such protons may be assigned to the ones of the HS forming the rigid domains. The dipolar couplings for proton pairs within these domains are not, or nearly not, averaged by reorientational motions, and thus result in a Gaussian-shaped relaxation component, with a fast decrease occurring over about 20 μs, typically, in the absence of any molecular mobility. The second term of eq 1 may be assigned to the protons from the PU soft domains. Well above their glass transition temperature, a significant part of the PU chain portions contributing to these domains displays fast and anisotropic reorientational motions, due to the topological constraints limiting them (cross-links, trapped entanglements, branching points, anchoring points to rigid

domains). As a result, both the $^1H$ dipolar couplings, related to the anisotropy of the segmental motions, and the $^1H$ $T_2$ relaxation time, related to the segmental fluctuations, are responsible for the transverse relaxation of the protons from such chain portions, as expressed by the terms $\exp(-q.M_2 \times t^2/2)$ and $\exp(-t/T_2)$, respectively, in eq 1. It may be noted that the occurrence of chain portions with anisotropic segmental dynamics in the soft domains makes the second term of eq 1 different from a pure exponential decay. In a first step, the parameters $q.M_2$ and $T_2$ are only used to provide a phenomenological description of the $^1H$ transverse relaxation decay in the time interval between about 40 μs and 200 μs, for which mobile protons only contribute to the measured signal.

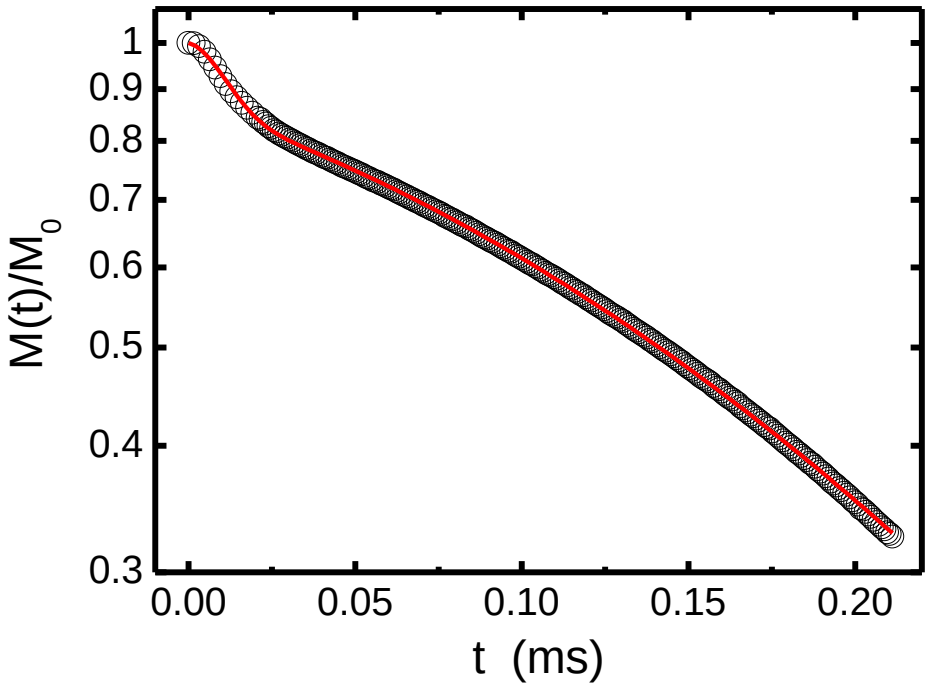


**Figure 4.** $^1H$ transverse relaxation signal determined at 80°C for PU1, using the Magic-Sandwich Echo pulse sequence. The solid line (—) corresponds to the fit of the experimental data using eq 1.

As shown in **Table S2**, the $T_2(^1H)$ values deduced from the fits of the $^1H$ MSE signals using eq 1 are somehow shorter than the ones that may be determined using the $^1H$ Hahn echo experiment, which are of the order of a few milliseconds at the temperature considered. Such a difference origins from the fact that in contrast to the Hahn echo pulse sequence, the MSE approach does not refocus the contributions of several effects which induce a faster $^1H$ transverse relaxation decay. Among them, one may cite the NMR magnetic field inhomogeneities, the diamagnetic susceptibility effects, occurring at the polymer/filler interfaces for instance, and the presence of protons with distinct $^1H$ chemical shift values. A more detailed analysis of the molecular motions within the PU soft domains will be performed in the following.

For the PU1 system, $f_H$ was found to be 13.0 % (± 0.3 %). A similar value of $f_H$ was derived for the three other polyurethanes: $f_H$ was indeed found to range between 13.0 % (± 0.3 %) and 15.5 % (± 0.3 %) (see Supplementary Information, **Figure S3** and **Table S2**). This result is consistent with the fact that the proportion of HTPB, chain extenders and IPDI is the same for the four systems: only the nature and the concentration of the catalyst and the curing conditions differ. Besides, the measured values of $f_H$ are consistent with the estimation based on the polyurethane composition and the proton density related to the components involved in the rigid domains (IPDI, chain-extender alcohols). Such an estimate indeed leads to $f_H$ = 13.5 %, as detailed in **Table S3**.

Let us now consider the soft domains, mainly composed of the HTPB chains. These latter display a network-like structure since their segmental motions are constrained by three kinds of topological constraints: rigid domains formed by the HS, HTPB branching points and trapped entanglements. In the following, the topology of these HTPB-based domains will be investigated for the polyurethane PU1, obtained after curing at 65°C. In a second step, the influence of the nature and the amount of catalyst as well as the curing temperature will be addressed. At this stage,

it is worth noting that the bulk samples which will be investigated in this section were all collected on EPDM/PU assemblies, far from the interface with the EPDM layer.

The network topology formed by the HTPB chains and, in particular, the molecular weight between two topological constraints ($M_c$), was determined by means of $^1$H DQ-based experiments. The analysis of such measurements was described in details in [12] and the different steps used to obtain the normalized DQ build-up curve $I_{DQ}(t_{DQ})$, based on the raw data recorded at 80°C, are illustrated for PU1 on **Figure S4**. The curve $I_{DQ}(t_{DQ})$ thus-obtained, depicted in **Figure 5**, does not depend on the measurement temperature, at least above 50°C, as illustrated in **Figure S5**. This feature indicates that the growth rate of the $^1$H DQ coherences may be interpreted as a result of the distribution $P(D_{res})$ of the $^1$H-$^1$H residual dipolar coupling $D_{res}$ ($D_{res}$ being inversely proportional to $M_c$), related to the chain portions constrained by the three kinds of topological constraints, either rigid domains, branching points or trapped entanglements, which may be considered as frozen over the millisecond time scale.

It is interesting to determine the $^1$H-$^1$H dipolar coupling values involved in the soft regions of the polyurethanes since these latter are directly proportional to the density of topological constraints which restrict the motions of the chain portions and in this respect, play an important role in the elastic behavior of these materials. The description of the build-up curve $I_{DQ}(t_{DQ})$ obtained for PU1 using the expression derived for a single $D_{res}$ value:

$$I_{DQ}(t_{DQ}, D_{res}) = \frac{1}{2}\left(1 - e^{-(0.378\, D_{res}\, t_{DQ})^{1.5}} \times \cos(0.583\, D_{res}\, t_{DQ})\right) \qquad (2)$$

is not satisfactory (see **Figure 5**) and as a result, a distribution of $D_{res}$ was used. In particular, attempts to use symmetrical distributions $P(D_{res})$, such as the Gaussian one, did not allow to account for the $I_{DQ}(t_{DQ})$ curve accurately. These fitting attempts suggested to use asymmetric

distributions and the log-normal distribution was found to be well-suited for the soft regions of PU1, as shown in **Figure 5**. The extension of the $P(D_{res})$ thus-obtained towards the low-$D_{res}$ (high-$M_c$) values indicates the presence of elastically-active chains displaying significantly higher $M_c$ values compared to most of the other chains of the same network.

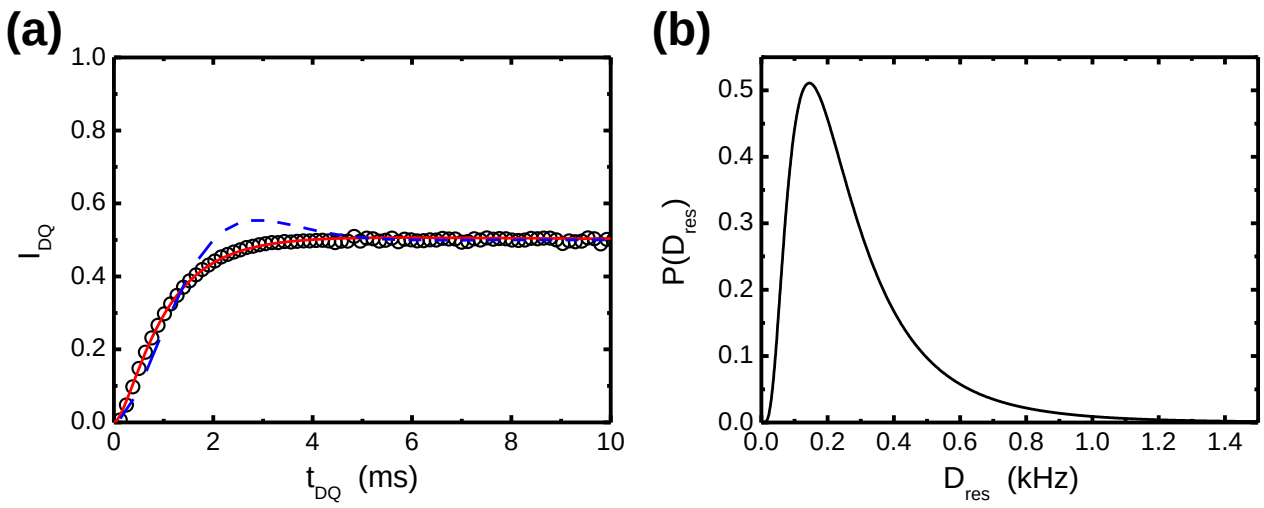


**Figure 5.** (a) Normalized $^1$H double-quantum (DQ) build-up curve for PU1 (bulk regions) at 80°C (○). The dashed line and the solid line are the fits of the experimental data using a single $D_{res}$ value (—) and a log-normal distribution of $D_{res}$, $P(D_{res})$ (—). (b) Log-normal distribution $P(D_{res})$ deduced from the $^1$H DQ NMR data reported in (a).

Another important feature to investigate the elastic behavior of the polyurethane materials is the fraction of elastically-active chains within the soft domains. This latter may be derived from the analysis of the reference signal, $S_{Ref}(t_{DQ})$, recorded through the $^1$H DQ NMR experiments. More precisely, prior to the normalization of the build-up of the DQ coherences, $S_{DQ}(t_{DQ})$, by the

sum [$S_{DQ}(t_{DQ})$ + $S_{Ref}(t_{DQ})$] to determine the normalized build-up $I_{DQ}(t_{DQ})$, $S_{Ref}(t_{DQ})$ should be subtracted from the contributions from the protons involved in the species freely diffusing in the network as well as the dangling chains. In the present case, the dangling chains may correspond to chain portions defined by a free end at one extremity and an anchoring point to a rigid domain or, alternatively, an entanglement or a HTPB branching point at the other extremity. For PU1, the reference signal $S_{Ref}(t_{DQ})$ measured at 80°C displays two decays above 5 ms, as shown in **Figure S4**: a slowly-relaxing component which may be identified above 26 ms and assigned to the sol species; an intermediate relaxation component, related to the dangling chain portions, which may be observed between 5 and 17 ms. Both decays may be described using an exponential function and the fraction of protons $f_{SOL}$ involved in the sol ($f_{DC}$ for the dangling chains, respectively) is deduced from the amplitude $A_{SOL}$ ($A_{DC}$ respectively) of the corresponding fit to the experimental data (see **Figure S4** and **Table S4**). Taking into account the fraction $f_H$ of protons located in the rigid domains, $f_{SOL}$ and $f_{DC}$ may indeed be expressed as:

$$f_{SOL} = (1 - f_H) \times \frac{A_{SOL}}{[S_{DQ}(t = 0\ s) + S_{Ref}(t = 0\ s)]}, f_{DC} = (1 - f_H) \times \frac{A_{DC}}{[S_{DQ}(t = 0\ s) + S_{Ref}(t = 0\ s)]} \quad (3)$$

For PU1, $f_H$ was found to be 13.0 % (± 0.3 %), so that $f_{SOL}$ and $f_{DC}$ may be thus estimated to 3.4 % (± 0.1 %) and 9.0 % (± 0.4 %), respectively. Correspondingly, the fraction of protons involved in the elastically-active chains amounts to 74.6 % (± 0.8 %). Taking into account the content of IPDI and chain extenders in PU1 prior to the formation of the urethane groups, one may estimate the expected fraction of protons which should not display significant reorientational motions over the tens of microseconds time scale, once involved in the rigid domains. As mentioned earlier, a percentage of about 13.5 % was obtained, which is very close to $f_H$ ($f_H$ = 13.0 %), determined by the MSE measurements. This feature suggests that the soft domains are mainly composed of

butadiene repeat units from HTPB and that the fraction of dilute HS in the soft domains may be neglected. Therefore, the network-like structure of PU1 may be considered as consisting in a distribution 75 % / 9 % / 3 % of butadiene repeat units involved in elastically-active chain portions, dangling chains and unentangled free chains. Lastly, it should be noted that the sol fraction $f_{SOL}$, deduced from these NMR measurements, is lower than the one determined using swelling experiments (**Table 1**). Indeed, only short, unentangled free HTPB chains and low-molecular-weight molecules contribute to $f_{SOL}$. The extractable fraction deduced from swelling measurements should also include long, entangled free chains as well as uncrosslinked chains involved in rigid domains formed by the HS.

### 3.4.2. Influence of the curing conditions

Similar $^{1}$H solid-state NMR approaches were used to probe the other materials, PU0, PU2 and PU3, thus allowing to evaluate the influence of the curing conditions – nature and amount of catalyst, curing temperature – on the polyurethane network topology. The fractions of each kind of network components are reported in **Table S4** and **Table S5** and the normalized $^{1}$H DQ build-up curves, $I_{DQ}(t_{DQ})$, measured for the different systems are shown in **Figure 6**.

The comparison between PU0 and PU1 indicates that the chemical nature of both catalysts considered in this work does not influence the network structure. The fractions of elastically-active chain portions, dangling chains and unentangled free chains are very similar for both materials (**Table S5**) while the distribution of the molecular weight between topological constraints, $M_c$, remains the same, as evidenced by the superimposition of both $I_{DQ}(t_{DQ})$ curves (**Figure 6a**). From another point of view, the $^{1}$H DQ NMR data obtained for PU2 and PU3 (**Figure 6b** and **Table S5**), which were both cured at 30°C, demonstrate that the amount of catalyst introduced in the initial mixture, before curing, does not play a significant role on the final structure of the polyurethane

network. Lastly, the curing temperature was varied between 65°C (PU1) and 30°C (PU2). As can be seen on **Figure 6c**, the evolution of $I_{DQ}$ with $t_{DQ}$ differs for both systems and in particular, the growth rate of the DQ coherences is weaker for PU2. Such a variation indicates that the elastically-active chains within PU2 display lower $D_{res}$ and thus, higher $M_c$-values than the ones within PU1. Besides, **Table S5** shows that the fraction of butadiene repeat units contributing to these network chains remains nearly the same, within the experimental accuracy, for both polyurethanes. Therefore, the combination of both features indicates that the reduction of the curing temperature leads to the formation of a network composed of a lower quantity of elastically-active chains, which are nevertheless longer, thus involving a constant overall number of repeat units.

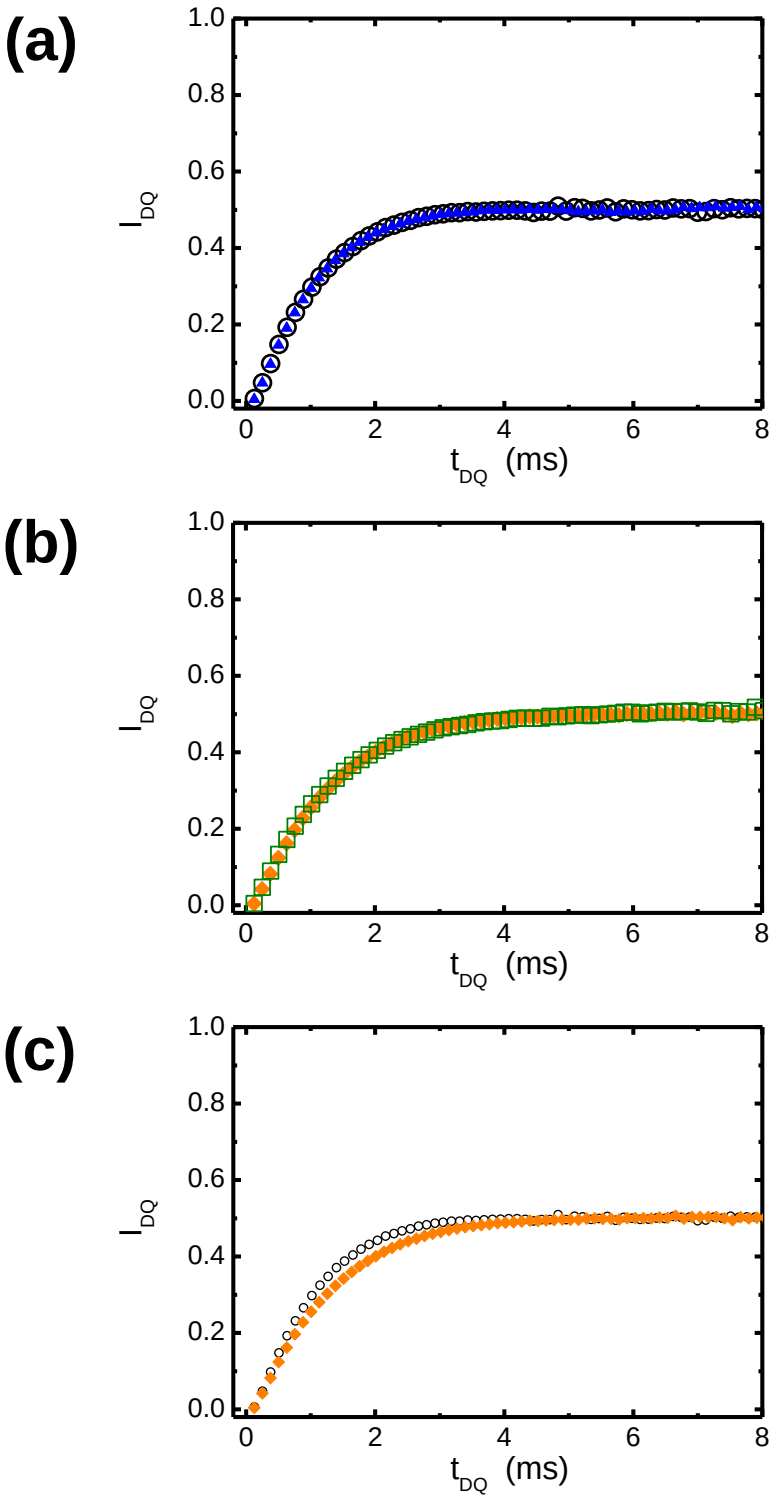


**Figure 6.** Comparison of the normalized $^{1}$H double-quantum build-up curves for the bulk regions of: (a) PU0 (▲) and PU1 (○), (b) PU2 (◆) and PU3 (□), (c) PU1 (○) and PU2 (◆).

### 3.5. Curing process near the interfaces with an EPDM substrate

The adhesion behavior of the polyurethane layer prepared on an EPDM substrate should strongly depends on its network structure and, in particular, the one close to the interface between both polymer components. Therefore, the PU topology was probed by means of the same $^{1}H$ solid-state NMR approaches as the ones used to study the bulk PU systems, the ones being located far from the interface with the EPDM component. However, in the present case, the experiments were carried out on 20 µm-thick slices, located in the PU side of the interfacial regions between the EPDM and the PU layers. Despite the rather limited total amount of slices obtained using a microtome (about 10 mg), such NMR measurements were possible because of the high intrinsic NMR sensitivity of $^{1}H$, combined with the use of a relatively high value of the NMR magnetic field (300 MHz), compared to low-field time-domain NMR equipments.

For each polyurethane, $^{1}H$ MSE experiments were performed on 20 µm-thick slices collected close to the EPDM component in order to determine the fraction of protons involved in the rigid domains, $f_H$, in this part of the PUs. As shown in **Figure S3** and **Table S2**, $f_H$ was found to be unchanged, within the experimental accuracy, for the four interfacial samples. Besides, these values, determined for the interphases, are also identical to the ones measured for the bulk regions (**Table S2**). This result indicates a homogeneous concentration of protons in the rigid zones formed by the HS, whatever the location from the EPDM substrate.

In the following, the PU network topology in the soft domains will be investigated for the interphases. **Figure 7a** shows the comparison of the $^{1}H$ DQ build-up curve obtained on the interfacial regions of PU1 and PU0, prepared at 65°C, under the same conditions: only the nature of the catalyst used for the urethane formation differs. The result obtained on the bulk regions of PU1 is also included in **Figure 7a**, for the sake of comparison. All the curves $I_{DQ}(t_{DQ})$ may clearly

be superimposed. Moreover, the fraction of protons involved in the elastically-active chains, the dangling chain portions and the sol remains similar for the interfacial zones of PU1, PU0 and the corresponding bulk regions (**Table S5**), within the experimental accuracy, which was estimated to ± 0.8 %, ± 0.4 % and ± 0.1 % respectively. Therefore, the network structure in the interfacial regions remains clearly identical, whatever the nature of the catalyst, and is also found to be unchanged compared to the one of the bulk regions of the same PU materials.

At this stage, it may be worth reminding that in the bulk polyurethanes, a reduction of the curing temperature from 65°C (PU1) down to 30°C (PU2) results in longer elastically-active chains, but involving the same total number of poly(butadiene) (PB) repeat units. As expected, the same trend is observed when the interfacial regions of PU1 and PU2 are selectively probed, as evidenced by **Figure 7b** and by the nearly constant fraction of protons related to the constrained chains for both interfacial materials (about 75 %, see **Table S5**). However, while the PU1 network topology formed at 65°C is homogeneous over several tens of micrometers length scale (identical $I_{DQ}(t_{DQ})$ curves for both interfacial and bulk regions, **Figure 7a**), one may observe that for PU2, prepared at 30°C, the variation of $I_{DQ}$ with $t_{DQ}$ measured close to the interface with the EPDM substrate display significant differences with the one determined in the bulk regions (**Figure 7b**). Indeed, from a qualitative aspect, the amplitude of the DQ coherences increases more slowly with the excitation time when interfacial regions are considered. More quantitatively, as for the bulk regions, the attempts to account for the $I_{DQ}(t_{DQ})$ curve using a symmetric distribution $P(D_{res})$ were not successful while an asymmetric, log-normal distribution of $D_{res}$ led to a satisfactory description of the experimental data (see **Figure 7b**). The corresponding distributions, compared in **Figure 7c**, show a significant decrease of the most probable $D_{res}$ value in the PU-side of the interface (73 Hz for the interfacial regions against 113 Hz for the bulk ones), together with the presence of

a lower fraction of protons displaying relatively high $D_{res}$ components (higher than 120 Hz, typically). Lastly, the amount of PB chain segments contributing to the elastically-active chains is rather similar for both interfacial and bulk zones (**Table S5**). As a result, the analysis of the $^{1}$H DQ NMR experiments demonstrates that as the formation of the urethane groups is performed at lower temperature (30°C), the resulting increase of the elastic network chain length is more pronounced close to the EPDM substrate than in the bulk PU2 material. Considering the thickness of the sample slices which were investigated in these NMR experiments, one may conclude that at 30°C, a gradient of the $M_c$ value occurs at the micrometer length scale, with a decreasing $M_c$ from the interface with EPDM towards the bulk regions. Such a gradient is not detected at 65°C (polyurethane PU1).

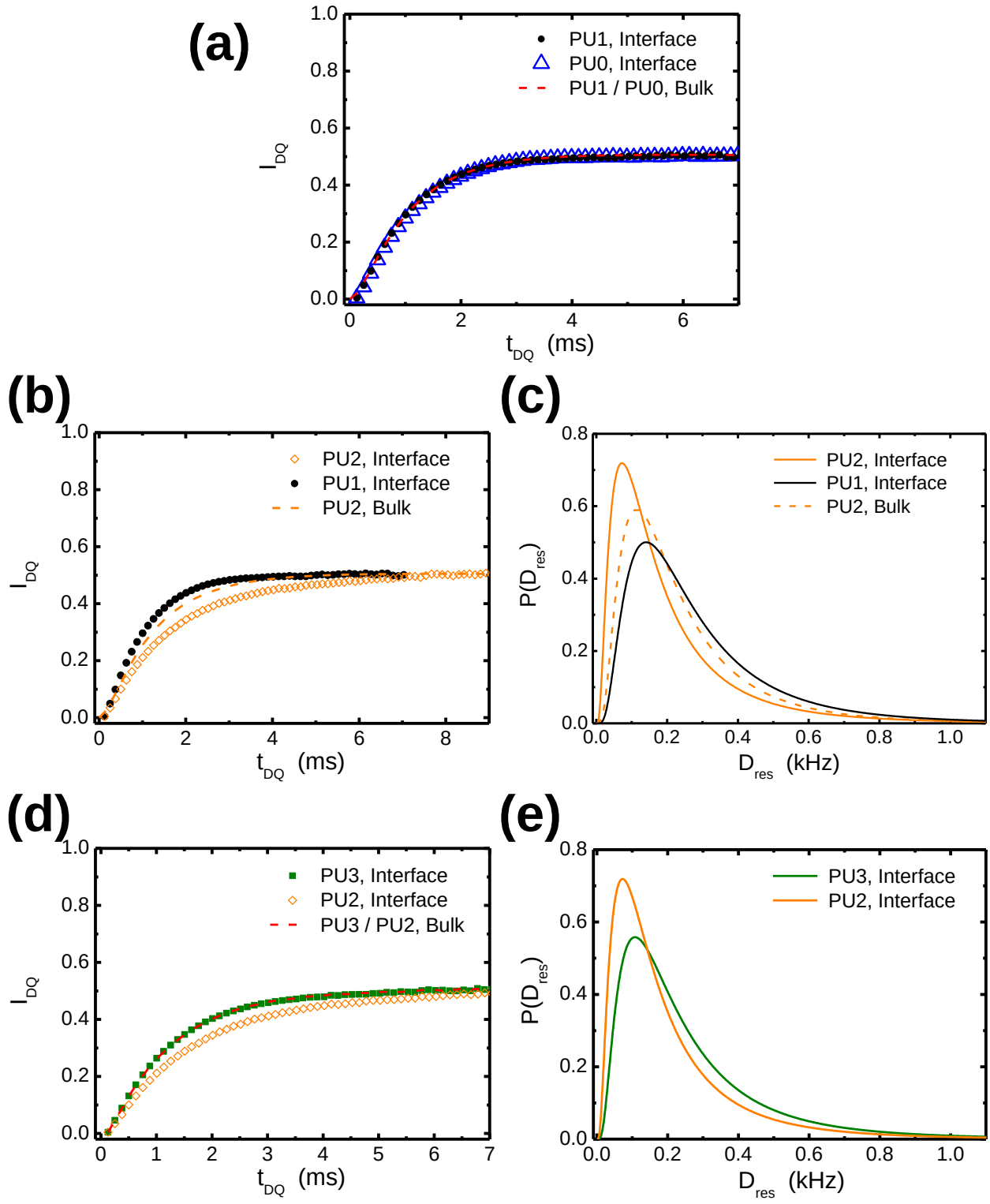


**Figure 7.** Influence of (a) the nature of the catalyst, (b), (c) the curing temperature and (d), (e) the catalyst concentration on the relative change of the PU network topology observed

between interfacial regions (close to the EPDM/PU interface) and bulk-like regions (500 μm away from the interface).

As for the bulk PU materials, the influence of the amount of catalyst used for the urethane group formation was evaluated at a curing temperature of 30°C. In the case of the interfacial PU regions, the fractions of protons involved in the elastic chains, the dangling chain portions and the unentangled free chains remain once again identical (**Table S5**) as the proportion of catalyst is multiplied by a factor ten (0.02 wt % for PU2 and 0.2 wt % for PU3). However, the $I_{DQ}(t_{DQ})$ curves for PU2 and PU3 slices located at the EPDM/PU interfaces are not identical, as illustrated in **Figure 7d**. The log-normal distribution of $D_{res}$, $P(D_{res})$, which were found to account for the experimental data obtained for both polyurethanes, are plotted in **Figure 7e**. An increase of the $D_{res}$ value at which the maximum of $P(D_{res})$ is reached – from 72 Hz to 108 Hz – is detected as the catalyst content is raised up. Moreover, a broadening of $P(D_{res})$ together with an extension towards the relatively high $D_{res}$ components are observed. All these features suggest that the topology of the network formed close to the interface is more strongly cross-linked as the amount of catalyst in the initial mixture, before reaction, is multiplied by ten. Such a behavior differs from the one displayed in the bulk regions of PU2 and PU3, for which the proportion of catalyst used was found to let the network structure of the soft domains unchanged. Interestingly, **Figure 7d** indicates that the higher catalyst content used to prepare PU3 leads to an identical network structure near the interface with EPDM and in the bulk, while for PU2 (lower amount of catalyst), weaker cross-linking densities were, on average, detected in the interfacial zones. The main results derived from the analysis of the solid-state NMR data shown in **Figure 7** are schematically summarized in **Table 2**.

| Sample | $M_{c,bulk}$ (g.mol$^{-1}$) | $M_{c,interface}$ (g.mol$^{-1}$) | Differences interface/bulk |
|---|---|---|---|
| **PU0** | 4520 | 4520 | No |
| **PU1** | 4520 | 4520 | No |
| **PU2** | 5800 | 8990 | Yes |
| **PU3** | 5800 | 5800 | No |

**Table 2.** Summary of the main results deduced from the analysis of the NMR data reported in **Figure 7**. $M_{c,bulk}$ and $M_{c,interface}$ correspond to the most probable molecular weight between topological contraints, determined far from and close to the EPDM/PU interface. These $M_c$ values were obtained using the distributions $P(D_{res})$ and the equation: $D_{res} = [656\ Hz.kg.mol^{-1}]/M_c$.[12]

## 4. DISCUSSION

Let us first quickly consider the network topology in the bulk of the PU materials considered in this work, which corresponds to the part far from the interface with the EPDM substrate. These systems will indeed serve as references for the description of the network structure in the interfacial regions with the EPDM component. The influence of the nature and the content of the catalyst as well as the reaction temperature were investigated. Among these parameters, the temperature was found to be the only one influencing the resulting density of topological constraints, which include anchoring points of the PB chain ends to domains formed by HS, branching points along the PB chains and trapped entanglements. As the composition of all the PUs investigated was identical, the difference in the density of topological constraints observed as the addition reaction temperature was varied between 30°C and 65°C might be, at least partly, assigned to a variation

in the extent of the urethane group formation. At this stage, it may be worthy recalling that the residual $^1H$ dipolar coupling $D_{res}$ is inversely proportional to $M_c$, the molecular weight between both topological constraints limiting the considered elastically-active chain portion. For PB-based networks, the constant of proportionality was estimated to 656 Hz.kg.mol$^{-1}$.[12] For the polyurethane prepared at 65°C (PU1), the most probable value of $D_{res}$, derived from the maximum of the distribution of $P(D_{res})$, is equal to $D_{res}$ = 145 Hz, which corresponds to $M_c \approx 4520$ g.mol$^{-1}$. When the formation of the PU network is performed at a lower temperature (30°C, PU2), $P(D_{res})$ displays a maximum for a weaker value of $D_{res}$ (113 Hz), related to a higher $M_c$ (about 5800 g.mol$^{-1}$). More generally, the comparison of the distributions $P(D_{res})$ derived on the polyurethane networks PU1 and PU2 indicates that the network prepared at 30°C (PU2) is composed of a higher proportion of long elastically-active chains, typically longer than 3680 g.mol$^{-1}$, than the one formed at 65°C (PU1). This latter value corresponds to the $M_c$ related to the intersection of both $P(D_{res})$ distributions.

From another point of view, the $M_c$ value for which $P(D_{res})$ reaches a maximum may be used to get a rough estimate of the Young modulus E of the polyurethane PU1, using the relationship:

$$E = \frac{3 \times d \times R \times T}{M_c} \quad (4)$$

with $d$, the density of PU1, assumed to be close to the PB density; $R$, the ideal gas constant and $T$, the temperature. Using $d$ = 0.91 g.cm$^{-3}$ and $T$ = 293 K, E may thus be estimated to about 1.5 MPa for PU1. As expected, this value is lower than the one deduced from the tensile test measurements, 6 MPa since the contribution from the filler particles (carbon black) was not taken into account in this estimate of E. When the formation of the PU network is performed under the same experimental conditions, but at lower temperature (30°C, PU2), the NMR results indicate that the

main fraction of the elastically-active chains are longer than the ones of PU1 while the number of PB repeat units involved by these chains remains the same. As a result, the Young modulus of PU2 is expected to be lower than the one measured for PU1, which is indeed the case, as shown by the stress-strain curves reported in **Figure 2**. This mechanical testing also shows identical behavior for PU0 and PU1, prepared at 65°C, as well as for PU2 and PU3, prepared at 30°C, again in agreement with the $^{1}$H DQ NMR results. The distribution $P(D_{res})$ was indeed found to be superimposed for PU0 and PU1 (**Figure 6a**) as well as for PU2 and PU3 (**Figure 6b**).

The following part of the discussion will focus on the PU elastomer topology at the interface of the EPDM layer. It should be first noted that the fraction of protons in the rigid domains formed by the HS remains nearly the same both in the interphase and in the bulk, whatever the PU system considered (see **Figure S3** and **Table S2**). Assuming that the characteristic size of these regions also keeps the same value whatever their distance from the interface with the EPDM substrate, the number of these topological constraints per unit volume should then be identical for both sample locations (interphase and bulk). This feature allows a direct comparison of the density of topological constraints for the chains within the soft domains in the interfacial and in the bulk regions. Such a comparison points out the occurrence of heterogeneities at the micrometer length scale when the PU network is synthesized at 30°C, with a quantity of the new catalyst equal to 0.02 wt % (PU2). Indeed, the PU2 network in the interfacial regions is composed of longer elastically-active chains than in the bulk part, with a $M_c$ value of about 8990 g.mol$^{-1}$, against 5800 g.mol$^{-1}$ far from the interface with EPDM. Both $M_c$ were obtained by considering the $D_{res}$ at the maximum of $P(D_{res})$ (**Figure 7c**). Moreover, the molecular weight $M_c$ between two topological constraints is found to be less distributed close to the EPDM layer than in the bulk, as evidenced by the narrower $P(D_{res})$. From the mechanical point of view, these features imply that the interfacial

regions of PU2 correspond to soft layers, characterized by a local elastic modulus $E_{int}$ which can be roughly estimated using eq 4 : $E_{int}$ = 0.7 MPa, against E = 1.2 MPa in the bulk PU2. Such a reduction of the local elastic modulus close to the EPDM substrate allows to rationalize the debonding of the PU2 layer occurring during the mechanical testing reported in **Figure 3**.

Interestingly, when the PU synthesis is carried out at 30°C, but with a higher amount of catalyst (0.2 wt %, system PU3), the adhesion between the PU and the EPDM layers significantly differs from the one observed for PU2/EPDM (**Figure 3**). In particular, the peak stress occurs for a higher value of the strain for PU3 than for PU2 and the plateau stress disappears for PU2. In this respect, the behavior displayed by PU3 is similar to the one determined for PU0 and PU1. Correspondingly, the $^{1}$H DQ NMR experiments clearly evidence that for PU3, the distribution of the molecular weight $M_c$ between two topological constraints close to the interface with the EPDM layer again becomes identical to the one in the bulk (**Figure 7e**), as for the samples prepared at 65°C (PU0 and PU1). Therefore, the NMR data suggest that from the mechanical point of view, the local elastic modulus related to the PU3 interphase should be identical to the one in the bulk and as for PU0 and PU1, this condition allows to prevent debonding of the PU layer at too low strain values (**Figure 3**). More generally, these results show that while the elastic behavior of the PU elastomers observed on **Figure 2** is consistent with the $^{1}$H NMR DQ measurements of the bulk regions, the adhesion performances of the PU layers at the interface with the EPDM substrate (**Figure 3**) may be rationalized by the network topology in the interphase as well as the local elastic modulus that may be estimated by solid-state NMR. The NMR approaches used in this study thus offer a unique avenue to get a selective description of the PU network within the interfacial regions, at the macromolecular length scale, which allows a deeper understanding of the adhesion behavior, at the macroscopic level.

As mentioned above, the difference of the network topology between the interfacial region and the bulk, observed when the PU elastomer is prepared with 0.02 wt % of catalyst, is not detected any longer when the same reactions are performed at the same temperature, but with a higher catalyst concentration $c_{cat}$ (0.2 wt %). Such a result may be rationalized by a transition occurring within the interphase between a control of the PU elastomer formation by diffusion at low $c_{cat}$ and a control by the reaction kinetics at high $c_{cat}$. Indeed, at 30°C, the use of a low amount of catalyst results in a slowing-down of the addition reactions. Therefore, under these conditions, the diffusion rate of the catalyst from the PU interfacial regions towards the EPDM substrate may be of the order of, or higher than the reaction rate. This diffusion process leads to a decrease of the local concentration of catalyst in the PU layer at the interface and a lower density of topological constraints is on average obtained. Increasing $c_{cat}$ up to 0.2 wt % leads to a speeding-up of the reaction kinetics so that the formation of the PU elastomer gets fast enough to limit the effect of diffusion towards the EPDM layer that occurs at the same time. In that case, the value of $c_{cat}$ in the interphase remains nearly unchanged during the network formation and the process is now controlled by the reaction kinetics. A similar competition between diffusion and reaction kinetics should also apply for IPDI.[26]

The diffusion of HTPB chains, IPDI and the other reaction components from the upper side of the cross-linked EPDM sheet into its bulk should occur over a characteristic length scale of at least 40 – 50 Å from the initial EPDM/HTPB interface.[27] As the polyaddition occurs, the PU elastomer chains are not only formed in the layer deposited on the EPDM substrate, but also in the part of the interphase located below the upper face of the EPDM sheet. Part of the PU elastomer network is thus formed among cross-linked EPDM chains. This structure is very important to ensure bonding between both elastomers (PU and EPDM), at the macroscopic length scale.

Nevertheless, the physical interactions that may be developed between both EPDM and PU network chains are somehow very limited, since these elastomers are incompatible.

## 5. CONCLUSIONS

Polyurethanes (PUs) obtained by using a hydroxyl-terminated poly(butadiene) oligomer (HTPB) and isophorone diisocyanate (IPDI) were prepared under various conditions on an EPDM substrate. The composition of all the elastomers investigated was kept unchanged and only the nature of the catalyst, its concentration and the reaction temperature were modified. In a first step, the kinetics of the network formation was monitored by viscosity measurements. In a second step, two kinds of mechanical testing were carried out: tensile tests on bulk PU systems, prepared under the same conditions, but without any EPDM layer, which enable to probe the elasticity of the global network; tensile tests on the assembly of both elastomeric layers (EPDM and PU), which aim at probing the adhesion behavior of the formed PU networks. In a last step, the PU network topology was investigated using $^{1}H$ solid-state NMR: the fraction of protons in the domains formed by the HS as well as the fraction of the elastically-active poly(butadiene) chains and the distribution of the molecular weight between topological constraints in the soft domains were determined.

In the case of the bulk PU elastomers (far from the EPDM layer), the nature as well as the concentration of catalyst were not found to influence their final bulk organization. The addition temperature is the only parameter which plays a role in the resulting cross-linked structure: as the reaction temperature gets lower, the network is characterized by a similar number of repeat units in the elastically-active chains, but these latter are on average longer, a feature which results in a

lower elastic modulus. In this respect, $^{1}H$ solid-state measurements and tensile test on bulk PUs were in total agreement.

The most salient result concerns the distribution of the molecular weight between topological constraints measured close to the interface with the EPDM layer. As the reaction temperature is high enough (65°C), this distribution and the fraction of elastically-active chains do not depend on the distance from the EPDM substrate, independently of the nature of the catalyst. In contrast, as the formation of the PU network is carried out at a lower temperature (30°C) while keeping the catalyst concentration unchanged (0.02 wt %), the network structure in the interfacial regions with EPDM differs from the one in the bulk: the $M_c$ values become significantly higher while the total number of repeat units in the elastically-active chains remains identical. Such a variation in the network topology suggests the occurrence of a lower value of the local elastic modulus than the one found further from the interface. From a mechanical point of view, such heterogeneities in the distribution of the density of the topological constraints along the normal to the interface result in debonding for a weaker value of the strain than for the PU prepared under the very same conditions, but at higher temperature (65°C). Interestingly, a ten time increase of the catalyst concentration leads to suppress the gradient of the topological constraint density from the interface towards the bulk regions. This feature is assigned to the transition from a network formation controlled by the diffusion at the interface to a control by the reaction kinetics. Interestingly, these observations, performed at the molecular length scale, are consistent with the level of adhesion performance recovered as the catalyst concentration is raised up from 0.02 wt % to 0.2 wt %.

In a more general way, this work demonstrates the possibility to account for the adhesion behavior of elastomers by using a description at the molecular level. At this stage, it may be worth noting that the approach used in this work remains valid for any other kinds of PU elastomers.[28]

Only the temperature at which the NMR experiments will be performed should be adapted to ensure that the segmental motions related to the α-relaxation of the chain portions in the soft domains are thermally activated over a characteristic time scale lower than the $^{1}H$ DQ excitation time $t_{DQ}$, i.e. a few milliseconds typically. Besides, due to its high sensitivity, $^{1}H$ solid-state NMR provides a unique opportunity to probe the network structure within the interfacial regions between two elastomer layers, the thickness of which was equal to 20 μm in the present work. The high sensitivity of these NMR approaches might even provide the avenue to determine the evolution of the network topology from the interface towards the bulk PU and therefore, the characteristic thickness of the interphase, by considering slices systematically collected along the normal to the EPDM/PU layers. The spatial resolution of such a profile, determined by the microtome characteristics, could be reduced to few micrometers.

ASSOCIATED CONTENT

**Supporting Information**.

The following files are available free of charge.

FTIR spectrum and XPS data for the surface of the EPDM substrate on which the PUs were prepared (**Figure S1**); Experimental device used for adhesion measurements and location of the collected PU samples investigated by $^{1}$H solid-state NMR (**Figure S2**); $^{1}$H solid-state NMR MSE experiments for PU0, PU2 and PU3, far and close to the interface with the EPDM substrate (**Figure S3**); $^{1}$H DQ experiments: Step-by-step description of the corrections of the $S_{Ref}$ data and the normalization procedure used to derive $I_{DQ}$ from $S_{DQ}$ and the corrected $S_{Ref}$, illustrated in the case of PU1 (**Figure S4**); Comparison of the normalized $^{1}$H DQ build-up curves obtained for PU0 (bulk regions) at 80°C and 100°C (**Figure S5**); Chemical structure of hexene-2-1-type, vinyl-type and geraniol-type hydroxyl groups found along the HTPB chains (**Scheme S1**); Adhesion properties of the EPDM/PU materials prepared with the four different PUs (**Table S1**); Fitting parameters obtained for the $^{1}$H MSE signal of the PU samples using eq 1 (**Table S2**); Estimation of the fraction of protons in the HS, deduced from the polyurethane composition (**Table S3**); Parameters describing the shape of $P(D_{res})$ (log-normal distribution), the fractions of PB repeat units involved in the dangling chain portions and the unentangled free chains for the PU materials (bulk and interphase) and their corresponding relaxation time $T_2$, as deduced from the $^{1}$H DQ experiments (**Table S4**); Fraction of protons involved in the rigid domains, the elastically-active chains, the dangling chain portions and the free extractables, deduced from the combination of $^{1}$H MSE and $^{1}$H DQ NMR experiments (**Table S5**).

AUTHOR INFORMATION

**Corresponding Authors**

Nancy Desgardin – Centre de Recherches du Bouchet (CRB), ArianeGroup, 9 rue Lavoisier 91710 Vert-le-Petit, France; E-mail: nancy.desgardin@ariane.group

Cédric Lorthioir – Laboratoire de Chimie de la Matière Condensée de Paris (LCMCP), UMR 7574 CNRS / Sorbonne Université, Sorbonne Université, 75005 Paris, France; orcid.org/0000-0001-8081-1601; E-mail: cedric.lorthioir@sorbonne-universite.fr

**Author**

Agnès Aymonier – ArianeGroup, Rue de Touban, Les Cinq Chemins, 33185 Le Haillan, France

**Author Contributions**

The manuscript was written through contributions of all authors. All authors have given approval to the final version of the manuscript.

**Notes**

The authors declare no competing financial interest.

ACKNOWLEDGMENTS

The authors are grateful to the French Procurement Agency (DGA) for financial support. C.L. thanks the Region Ile-de-France for its contribution to the acquisition of the solid-state NMR spectrometer, in the framework of DIM Nano-K.

ABBREVIATIONS

PU, polyurethane; EPDM, ethylene-propylene-diene rubber; NMR, nuclear magnetic resonance; MSE, magic-sandwich echo; DQ, double-quantum.

REFERENCES


(1) Léger, L.; Creton, C. Adhesion Mechanisms at Soft Polymer Interfaces. *Philos. Trans. R. Soc. Math. Phys. Eng. Sci.* **2008**, *366* (1869), 1425–1442. https://doi.org/10.1098/rsta.2007.2166.

(2) Creton, C.; Ciccotti, M. Fracture and Adhesion of Soft Materials: A Review. *Rep. Prog. Phys.* **2016**, *79* (4), 046601. https://doi.org/10.1088/0034-4885/79/4/046601.

(3) Raos, G.; Zappone, B. Polymer Adhesion: Seeking New Solutions for an Old Problem. *Macromolecules* **2021**, *54* (23), 10617–10644. https://doi.org/10.1021/acs.macromol.1c01182.

(4) Prisacariu, C. *Polyurethane Elastomers*; Springer: Dordrecht, **2011**.

(5) Yu, Y.; Sanchez, D.; Lu, N. Work of Adhesion/Separation between Soft Elastomers of Different Mixing Ratios. *J. Mater. Res.* **2015**, *30* (18), 2702–2712. https://doi.org/10.1557/jmr.2015.242.

(6) Zhou, Q.-C.; Xu, J.-S.; Chen, X.; Zhou, C.-S. Review of the Adhesively Bonded Interface in a Solid Rocket Motor. *J. Adhes.* **2016**, *92* (5), 402–428. https://doi.org/10.1080/00218464.2015.1040155.

(7) Akindoyo, J. O.; Beg, M. D. H.; Ghazali, S.; Islam, M. R.; Jeyaratnam, N.; Yuvaraj, A. R. Polyurethane Types, Synthesis and Applications – a Review. *RSC Adv.* **2016**, *6* (115), 114453–114482. https://doi.org/10.1039/C6RA14525F.

(8) Clayden, N. J.; Howick, C. Effect of the Processing Temperature on the Interaction between Plasticizer and Poly(Vinyl Chloride) as Studied by Solid State NMR Spectroscopy. *Polymer* **1993**, *34* (12), 2508–2515. https://doi.org/10.1016/0032-3861(93)90580-4.

(9) Yamasaki, S.; Nishiguchi, D.; Kojio, K.; Furukawa, M. Effects of Polymerization Method on Structure and Properties of Thermoplastic Polyurethanes. *J. Polym. Sci. Part B Polym. Phys.* **2007**, *45* (7), 800–814. https://doi.org/10.1002/polb.21080.

(10) Orza, R. A.; Magusin, P. C. M. M.; Litvinov, V. M.; van Duin, M.; Michels, M. A. J. Mechanism for Peroxide Cross-Linking of EPDM Rubber from MAS $^{13}$C NMR Spectroscopy. *Macromolecules* **2009**, *42* (22), 8914–8924. https://doi.org/10.1021/ma9016482.

(11) Asano, A. Chapter One - NMR Relaxation Studies of Elastomers. In *Annual Reports on NMR Spectroscopy*; Webb, G. A., Ed.; Academic Press, **2015**; *86*, 1–72. https://doi.org/10.1016/bs.arnmr.2015.04.001.

(12) Saalwächter, K. Proton Multiple-Quantum NMR for the Study of Chain Dynamics and Structural Constraints in Polymeric Soft Materials. *Prog. Nucl. Magn. Reson. Spectrosc.* **2007**, *51* (1), 1–35. https://doi.org/10.1016/j.pnmrs.2007.01.001.

(13) Saalwächter, K. Multiple-Quantum NMR Studies of Anisotropic Polymer Chain Dynamics. In *Modern Magnetic Resonance*; Webb, G. A., Ed.; Springer International Publishing: Cham, **2018**; 755–781. https://doi.org/10.1007/978-3-319-28388-3_59.

(14) Ducruet, N.; Delmotte, L.; Schrodj, G.; Stankiewicz, F.; Desgardin, N.; Vallat, M.-F.; Haidar, B. Evaluation of Hydroxyl Terminated Polybutadiene-Isophorone Diisocyanate Gel Formation during Crosslinking Process. *J. Appl. Polym. Sci.* **2013**, *128* (1), 436–443. https://doi.org/10.1002/app.38194.

(15) Maus, A.; Hertlein, C.; Saalwächter, K. A Robust Proton NMR Method to Investigate Hard/Soft Ratios, Crystallinity, and Component Mobility in Polymers. *Macromol. Chem. Phys.* **2006**, *207* (13), 1150–1158. https://doi.org/10.1002/macp.200600169.
(16) Vilar, W. D.; Menezes, S. M. C.; Akcelrud, L. Characterization of Hydroxyl-Terminated Polybutadiene. *Polym. Bull.* **1994**, *33* (5), 563–570. https://doi.org/10.1007/BF00296165.
(17) Litvinov, V. M. EPDM/PP Thermoplastic Vulcanizates As Studied by Proton NMR Relaxation: Phase Composition, Molecular Mobility, Network Structure in the Rubbery Phase, and Network Heterogeneity. *Macromolecules* **2006**, *39* (25), 8727–8741. https://doi.org/10.1021/ma061911h.
(18) Sekkar, V.; Raunija, T. S. K. Issues Related with Pot Life Extension for Hydroxyl-Terminated Polybutadiene-Based Solid Propellant Binder System. *Propellants Explos. Pyrotech.* **2015**, *40* (2), 267–274. https://doi.org/10.1002/prep.201400054.
(19) Panicker, S. S.; Ninan, K. N. Effect of Reactivity of Different Types of Hydroxyl Groups of HTPB on Mechanical Properties of the Cured Product. *J. Appl. Polym. Sci.* **1997**, *63* (10), 1313–1320. https://doi.org/10.1002/(SICI)1097-4628(19970307)63:10<1313::AID-APP10>3.0.CO;2-5.
(20) Ono, H.-K.; Jones, F. N.; Pappas, S. P. Relative Reactivity of Isocyanate Groups of Isophorone Diisocyanate. Unexpected High Reactivity of the Secondary Isocyanate Group. *J. Polym. Sci. Polym. Lett. Ed.* **1985**, *23* (10), 509–515. https://doi.org/10.1002/pol.1985.130231003.
(21) Eroğlu, M. S. Characterization of the Network Structure of Hydroxyl Terminated Poly(Butadiene) Elastomers Prepared by Different Reactive Systems. *J. Appl. Polym. Sci.* **1998**, *70* (6), 1129–1135. https://doi.org/10.1002/(SICI)1097-4628(19981107)70:6<1129::AID-APP9>3.0.CO;2-Q.
(22) Gui, D.; Zong, Y.; Ding, S.; Li, C.; Zhang, Q.; Wang, M.; Liu, J.; Chi, X.; Ma, X.; Pang, A. In–Situ Characterization and Cure Kinetics in NEPE Propellant/HTPB Liner Interface by Microscopic FT-IR. *Propellants Explos. Pyrotech.* **2017**, *42* (4), 410–416. https://doi.org/10.1002/prep.201600087.
(23) Callies, X.; Fonteneau, C.; Pensec, S.; Bouteiller, L.; Ducouret, G.; Creton, C. Adhesion and Non-Linear Rheology of Adhesives with Supramolecular Crosslinking Points. *Soft Matter* **2016**, *12* (34), 7174–7185. https://doi.org/10.1039/C6SM01154C.
(24) Kojio, K.; Nozaki, S.; Takahara, A.; Yamasaki, S. Influence of Chemical Structure of Hard Segments on Physical Properties of Polyurethane Elastomers: A Review. *J. Polym. Res.* **2020**, *27* (6), 140. https://doi.org/10.1007/s10965-020-02090-9.
(25) Desgardin, N.; Albigès, R.; Bouteiller, L.; Pensec, S. Hydrogen Bonds in HTPB and GAP Polyurethanes; 51st International Annual Conference of the Fraunhofer-Institüt für Chemishe Technologie: Karlsruhe, **2022**.
(26) Desgardin, N.; Ducruet, N.; Vallat, M.-F.; Vitrac, O. Diffusion Mechanism at the Liner Propellant Interface; 43rd International Annual Conference of the Fraunhofer-Institüt für Chemishe Technologie: Karlsruhe, **2012**. ISSN 2194-4903.
(27) Schach, R.; Tran, Y.; Menelle, A.; Creton, C. Role of Chain Interpenetration in the Adhesion between Immiscible Polymer Melts. *Macromolecules* **2007**, *40* (17), 6325–6332. https://doi.org/10.1021/ma0707990.
(28) Zhang, R.; Yu, S.; Chen, S.; Wu, Q.; Chen, T.; Sun, P.; Li, B.; Ding, D. Reversible Cross-Linking, Microdomain Structure, and Heterogeneous Dynamics in Thermally Reversible

Cross-Linked Polyurethane as Revealed by Solid-State NMR. *J. Phys. Chem. B* **2014**, *118* (4), 1126–1137. https://doi.org/10.1021/jp409893f.

**For Table of Contents use only:**

Title: Network Topology of the Interphase between Cross-linked Polyurethane/Ethylene Propylene Diene Terpolymer Elastomers for Adhesion Applications.

Authors: Desgardin, N.; Aymonier, A.; Lorthioir, C.

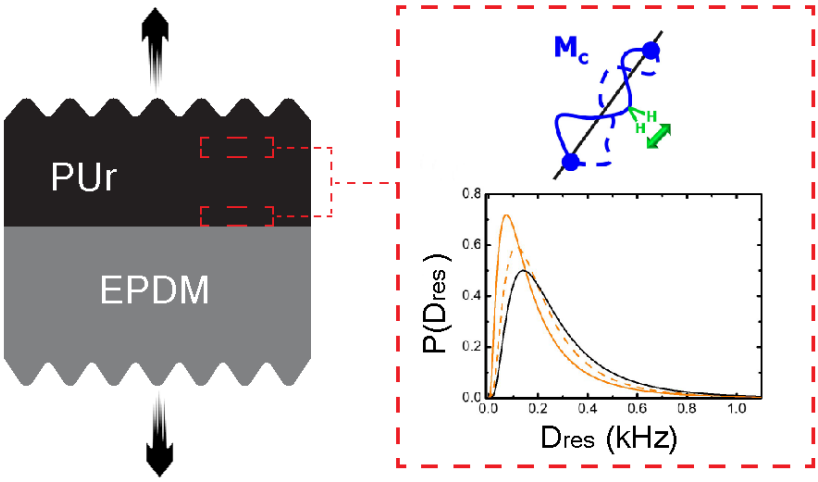

# Supporting Information

# Network Topology of the Interphase between Cross-linked Polyurethane/Ethylene Propylene Diene Terpolymer Elastomers for Adhesion Applications

*Nancy Desgardin*[1,*], *Agnès Aymonier*[1], *Cédric Lorthioir*[2,*]

(1) ArianeGroup, Centre de Recherches du Bouchet, 91710 Vert Le Petit, France

(2) Sorbonne Université, CNRS, Laboratoire de Chimie de la Matière Condensée de Paris, LCMCP, UMR 7574, 75005 Paris, France

* Corresponding authors ;

E-mail address : nancy.desgardin@ariane.group (Nancy Desgardin)

cedric.lorthioir@sorbonne-universite.fr (Cédric Lorthioir)

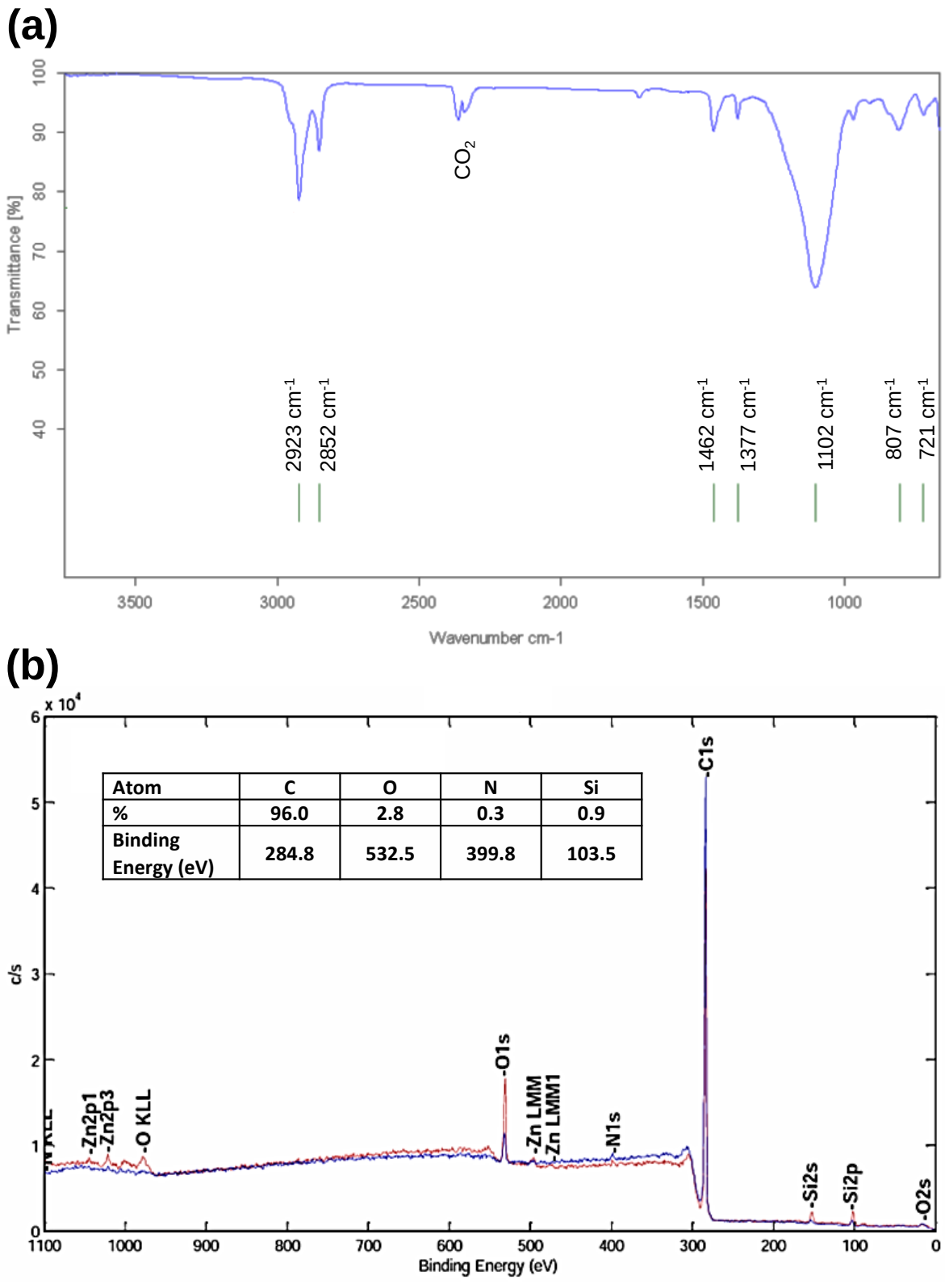


**Figure S1.** Characterization of the surface composition of the EPDM sheet on which the PU layers of the EPDM/PU assemblies were prepared: (a) FTIR spectrum obtained

using the ATR mode with a germanium crystal. This latter leads to a probed depth of about 0.6 μm at a wavenumber of 1000 $cm^{-1}$; (b) XPS spectrum (survey scan) and the corresponding composition.

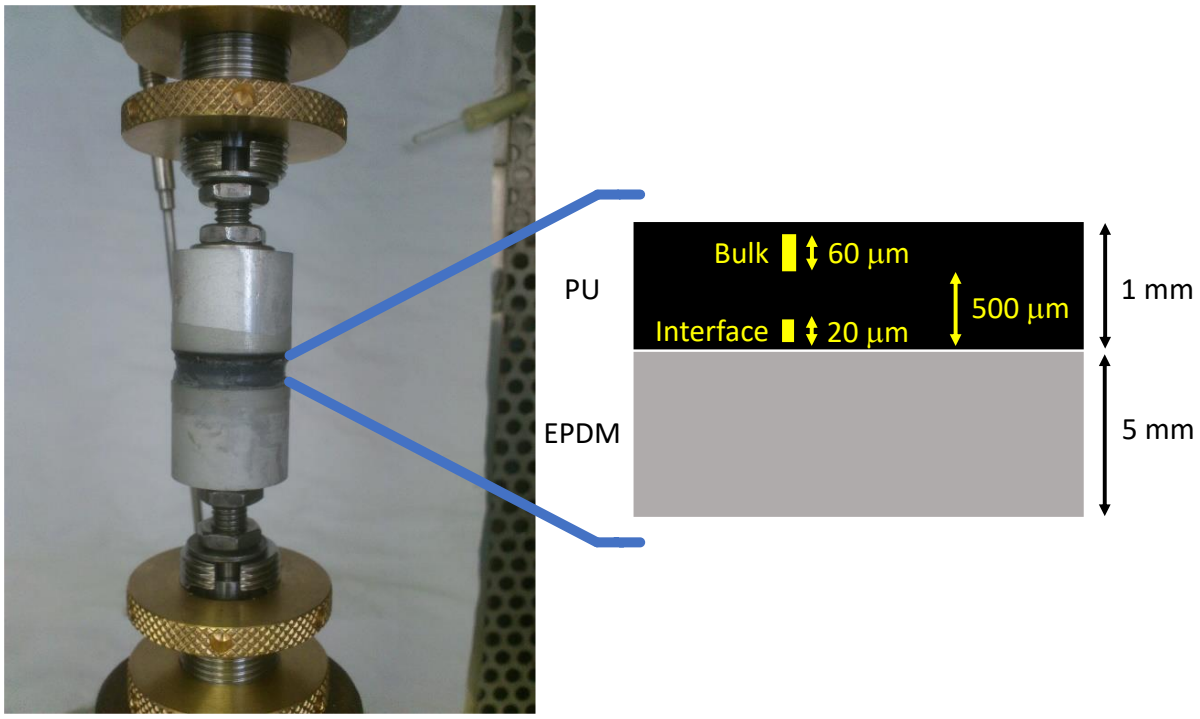


**Figure S2.** Mechanical set-up used to evaluate the adhesive properties of polyurethanes on an EPDM surface. The location of the microtomed slices used for the $^{1}H$ solid-state NMR experiments (interface and bulk domains) are schematically represented.

| Sample name | Cavitation stress (MPa) | Cavitation strain (%) | Stress at break (MPa) | Strain at break (%) | Energy ($J/cm^3$) |
|---|---|---|---|---|---|
| **PU0** | 4.3 / 4.1 / 4.3 | 22.2 / 24.4 / 19.5 | 3.9 / 4.1 / 3.6 | 129 / 145 / 105 | 5.2 / 5.3 / 4.0 |
| **PU1** | 4.6 / 4.1 / 4.2 | 20.3 / 22.6 / 21.9 | 5.1 / 5.0 / 5.7 | 221 / 213 / 252 | 9.1 / 8.3 / 10.6 |
| **PU2** | 3.6 / 3.5 / 3.5 | 14.3 / 14.1 / 14.4 | 3.1 / 3.1 / 3.1 | 23 / 24 / 29 | 0.9 / 0.9 / 1.1 |
| **PU3** | 4.6 / 4.3 / 4.7 | 16.8 / 19.7 / 18.3 | 4.0 / 4.3 / 4.1 | 135 / 181 / 160 | 5.3 / 6.9 / 6.2 |

**Table S1.** Adhesion properties of the EPDM/PU materials prepared with the four different PUs. For each system, the results obtained on three specimens are indicated.

**(a) PU0, Bulk**

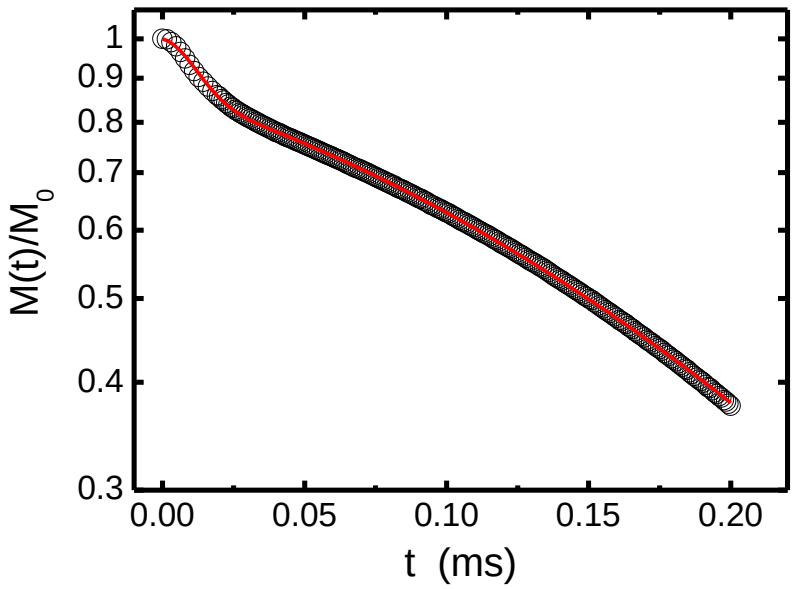


**PU2, Bulk**

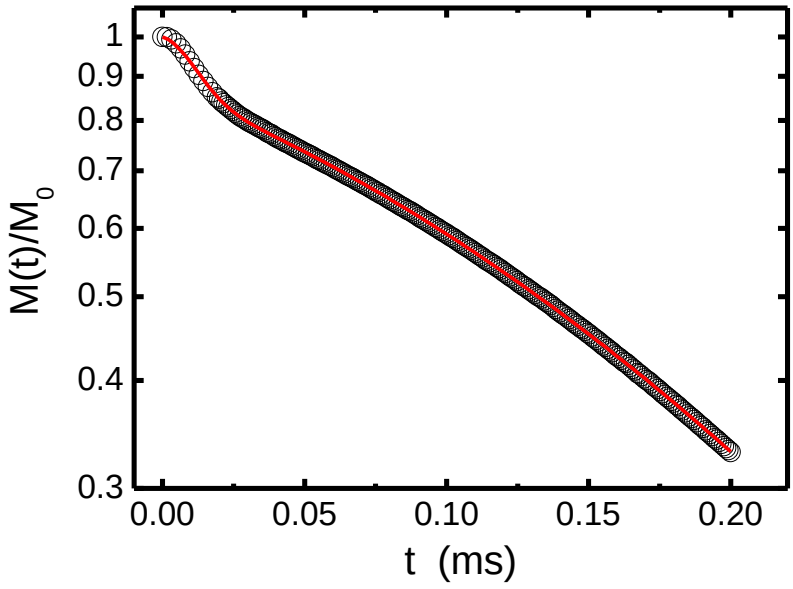


**PU3, Bulk**

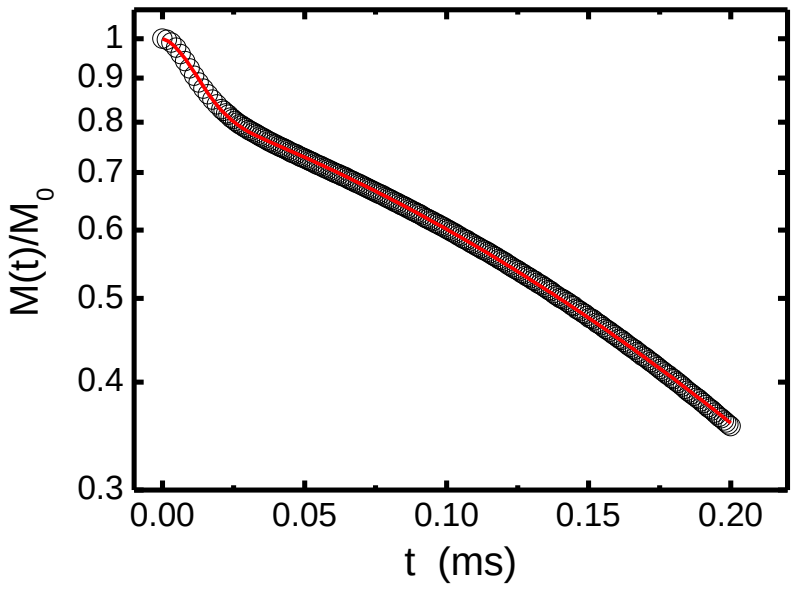

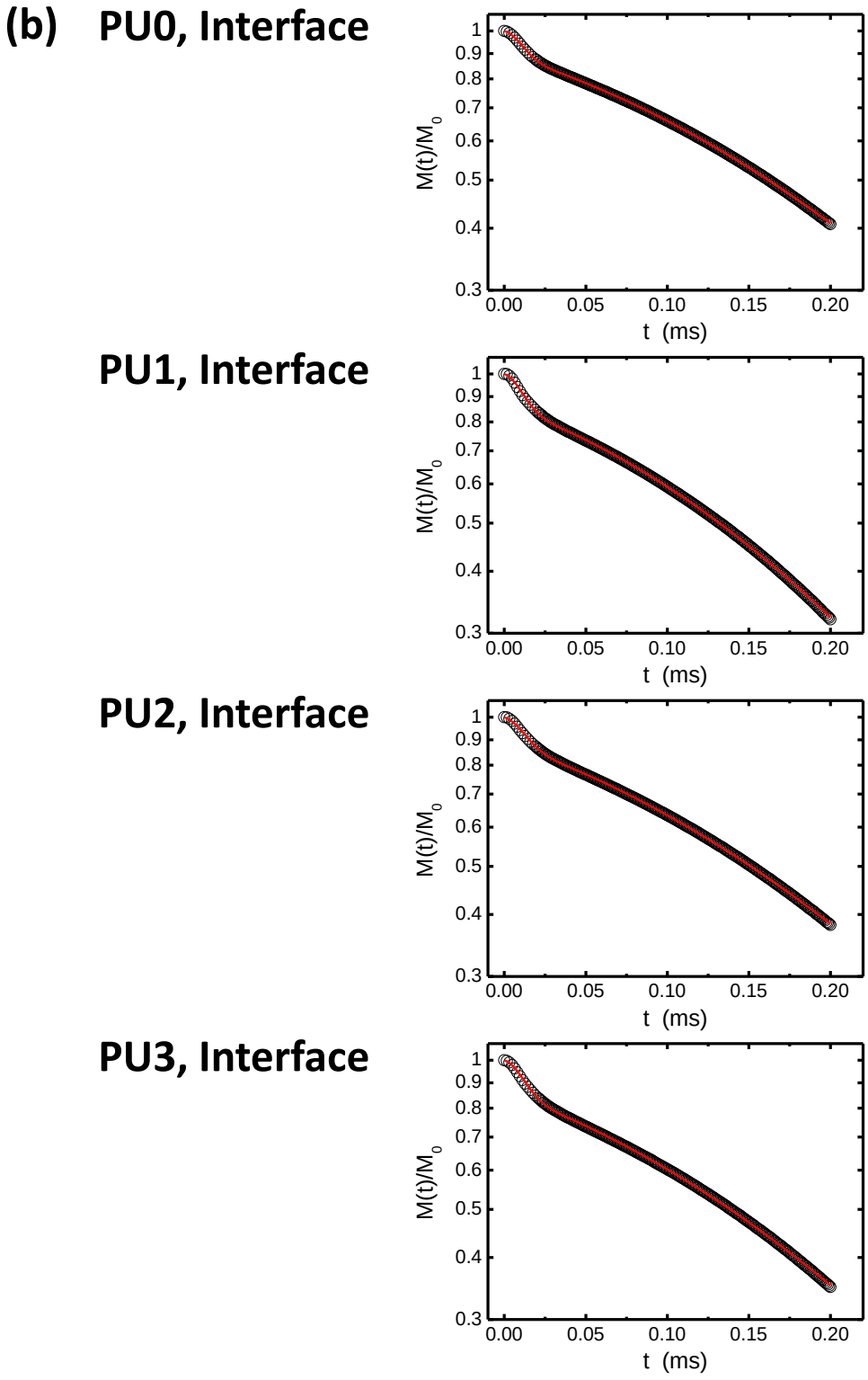


**Figure S3.** $^{1}$H transverse relaxation signals obtained for (a) PU0, PU2 and PU3 far from the EPDM substrate (bulk); (b) PU0, PU1, PU2 and PU3 at the interface with the EPDM layer. These measurements were carried out at 353 K, using the Magic-Sandwich Echo pulse sequence and a single MSE cycle.

| Bulk | $f_H$ (%) | a ($ms^{-2}$) | q.$M_2$ ($ms^{-2}$) | $T_2$ (ms) |
|---|---|---|---|---|
| **PU0** | 13.1 | 7847 | 18 | 0.43 |
| **PU1** | 13.0 | 9156 | 20 | 0.39 |
| **PU2** | 12.5 | 7805 | 19 | 0.33 |
| **PU3** | 15.5 | 8113 | 18 | 0.40 |

| Interphase | $f_H$ (%) | a ($ms^{-2}$) | q.$M_2$ ($ms^{-2}$) | $T_2$ (ms) |
|---|---|---|---|---|
| **PU0** | 10.2 | 9184 | 17 | 0.44 |
| **PU1** | 13.6 | 9284 | 23 | 0.38 |
| **PU2** | 11.0 | 7382 | 17 | 0.39 |
| **PU3** | 13.8 | 7946 | 18 | 0.37 |

**Table S2.** Parameters resulting from the fit of the $^1H$ transverse relaxation signals shown in **Figure S3**, by eq 1. The percent error on the value of the fraction $f_H$ of protons located in the PU hard domains is estimated to ±2 %.

| | |
|---|---|
| HTPB | 70.8 % mol H |
| IPDI | 17.4 % mol H |
| Diol chain extenders | 9.1 % mol H |
| Carbon black | 0.00 % mol H |
| Antioxidant | 0.70 % mol H |
| Bonding agent | 2 % mol H |
| Catalyst | negligible |

**Table S3.** Composition of the polyurethane PU0, allowing to estimate the fraction of protons for the moieties involved in the hard domains.

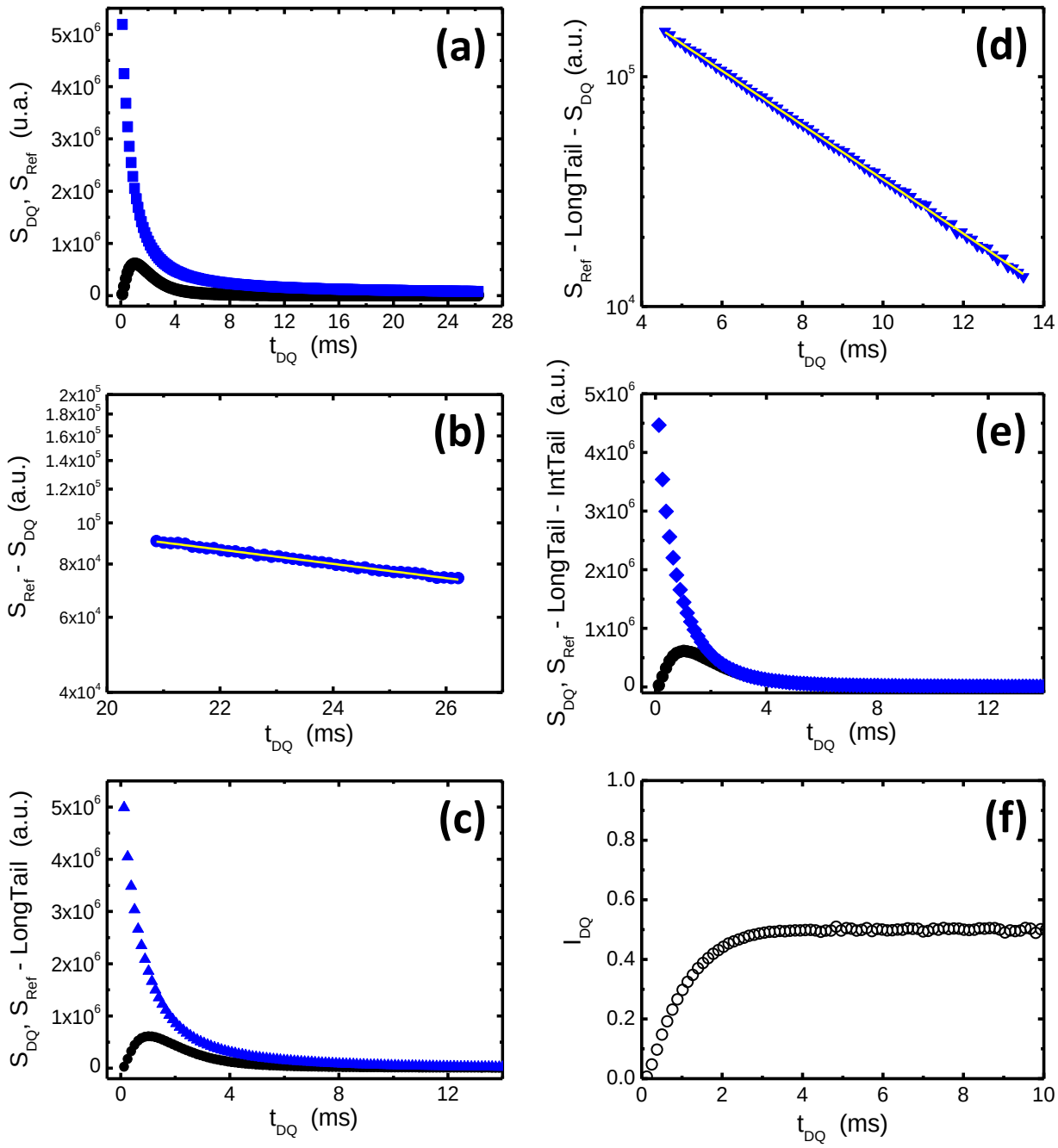


**Figure S4.** (a) Evolution of $S_{DQ}$ (●) and $S_{Ref}$ (■) with $t_{DQ}$, measured for PU1 at T = 353 K. (b) Fit of $[S_{Ref} - S_{DQ}](t_{DQ})$ in the long-time regime, using a single-exponential decay, $A_{SOL}\times\exp(-t_{DQ}/T_{2,SOL})$. The solid line corresponds to the fitting curve. (c) Variation of $S_{DQ}$ (●) and $[S_{Ref} - A_{SOL}\times\exp(-t_{DQ}/T_{2,SOL})]$ (▲) with $t_{DQ}$. (d) Fit of $[S_{Ref} - A_{SOL}\times\exp(-t_{DQ}/T_{2,SOL}) - S_{DQ}](t_{DQ})$ by a single-exponential decay ($A_{DC}\times\exp(-t_{DQ}/T_{2,DC})$), in the intermediate time range. The solid line stands for the fitting line.

(e) Comparison between $S_{DQ}(t_{DQ})$ (●) and $[S_{Ref} - A_{SOL}\times\exp(-t_{DQ}/T_{2,SOL}) - A_{DC}\times\exp(-t_{DQ}/T_{2,DC})](t_{DQ})$ (◆). This latter corresponds to the reference signal, $S_{Ref}(t_{DQ})$, subtracted by the contributions from the protons related to $^{1}H$-$^{1}H$ dipolar couplings averaged to zero, due to isotropic reorientational motions over the tens of microseconds time scale, at T = 353 K. (f) Normalized $^{1}H$ double-quantum build-up curve, $I_{DQ}(t_{DQ})$, determined by dividing $S_{DQ}(t_{DQ})$ by the corrected reference signal.

| Bulk | ln[$D_0$ (kHz)] | σ | $A_{SOL}$ (%) | $T_{2,SOL}$ (ms) | $A_{DC}$ (%) | $T_{2,DC}$ (ms) |
|---|---|---|---|---|---|---|
| **PU0** | -1.47 | 0.68 | 3.7 | 31.1 | 9.5 | 4.3 |
| **PU1** | -1.47 | 0.68 | 3.9 | 26.0 | 10.4 | 3.7 |
| **PU2** | -1.65 | 0.72 | 4.2 | 22.6 | 12.7 | 3.5 |
| **PU3** | -1.65 | 0.72 | 3.9 | 28.3 | 10.9 | 4.0 |

| Interphase | ln[$D_0$ (kHz)] | σ | $A_{SOL}$ (%) | $T_{2,SOL}$ (ms) | $A_{DC}$ (%) | $T_{2,DC}$ (ms) |
|---|---|---|---|---|---|---|
| **PU0** | -1.47 | 0.70 | 2.7 | 30.6 | 9.4 | 3.9 |
| **PU1** | -1.47 | 0.70 | 2.7 | 40.1 | 9.6 | 4.6 |
| **PU2** | -1.91 | 0.85 | 3.7 | 26.4 | 12.9 | 4.4 |
| **PU3** | -1.62 | 0.78 | 3.5 | 29.2 | 10.2 | 4.1 |

**Table S4.** Parameters describing the log-normal distribution of $D_{res}$, $P(D_{res}) = \frac{1}{\sigma\sqrt{2\pi}\,D_{res}}\, e^{-\frac{(\ln D_{res} - \ln D_0)^2}{2\sigma^2}}$. The fractions of protons present in the soft domains, belonging to dangling chain portions ($A_{DC}$) and unentangled free chains ($A_{SOL}$), are reported, together with their corresponding transverse relaxation time, $T_{2,SOL}$ and $T_{2,DC}$, determined using the reference signal $S_{Ref}(t_{DQ})$. The percent error on ln[$D_0$ (kHz)], σ, $A_{SOL}$, $T_{2,SOL}$, $A_{DC}$ and $T_{2,DC}$ is estimated to ±2 %, ±8 %, ±1 %, ±1 %, ±2 % and ±1 %, respectively.

| Bulk | $f_H$ (%) | $f_{EAC}$ (%) | $f_{DC}$ (%) | $f_{SOL}$ (%) |
|---|---|---|---|---|
| **PU0** | 13.1 | 75.4 | 8.3 | 3.2 |
| **PU1** | 13.0 | 74.6 | 9.0 | 3.4 |
| **PU2** | 12.5 | 72.7 | 11.1 | 3.7 |
| **PU3** | 15.5 | 72.0 | 9.2 | 3.3 |

| Interphase | $f_H$ (%) | $f_{EAC}$ (%) | $f_{DC}$ (%) | $f_{SOL}$ (%) |
|---|---|---|---|---|
| **PU0** | 10.2 | 78.9 | 8.5 | 2.4 |
| **PU1** | 13.6 | 75.8 | 8.3 | 2.3 |
| **PU2** | 11.0 | 74.1 | 11.5 | 3.4 |
| **PU3** | 13.8 | 74.4 | 8.8 | 3.0 |

**Table S5.** Fractions of protons involved in the rigid domains formed by the hard segments ($f_H$) and the different populations present in the soft domains: elastically-active chains ($f_{EAC}$), dangling chain portions ($f_{DC}$) and unentangled free chains ($f_{SOL}$). The percent error on $f_H$, $f_{SOL}$, $f_{DC}$ and $f_{EAC}$ is estimated to ±2 %, ±3 %, ±4 % and ±1 %, respectively.

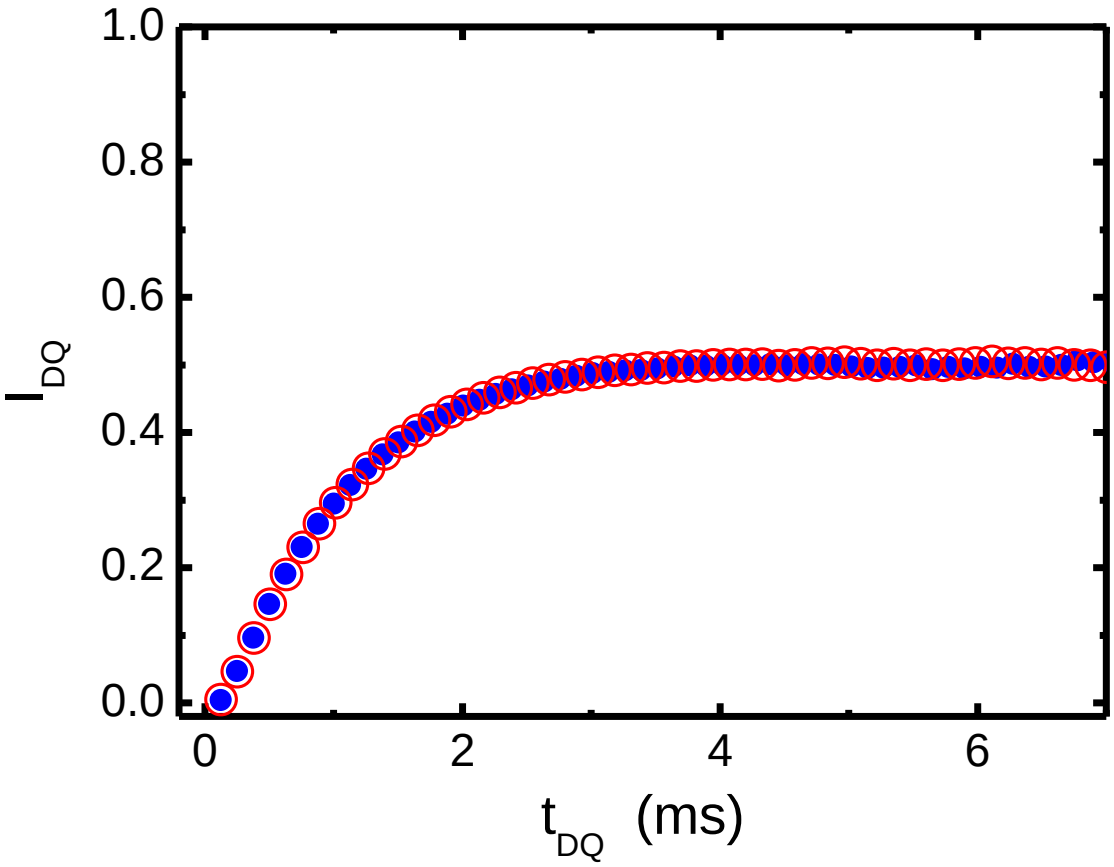


**Figure S5.** Comparison of the $^{1}$H DQ build-up curves, $I_{DQ}(t_{DQ})$, obtained for PU0 at T = 80°C (●) and 100 °C (○).

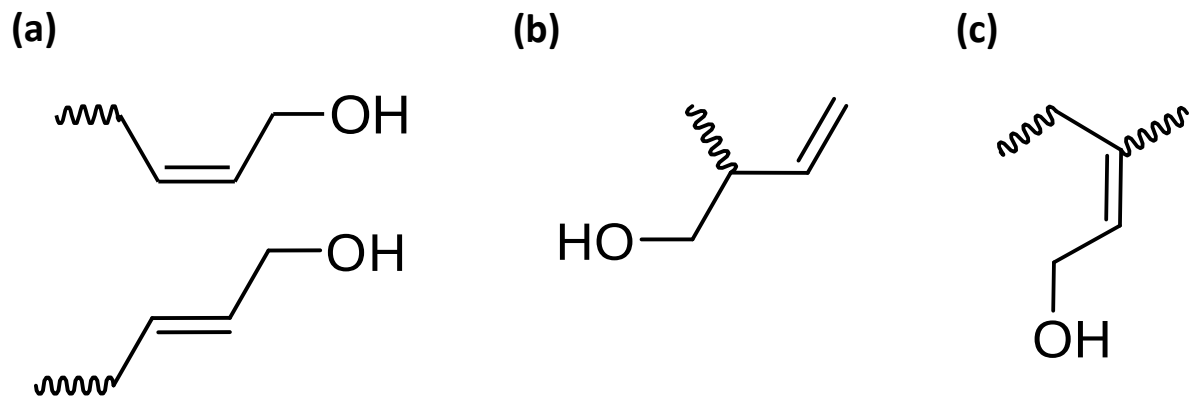


**Scheme S1.** Chemical structure of (a) hexene-2-1-type, (b) vinyl-type and (c) geraniol-type hydroxyl groups found along the HTPB chains.